Design of a Portable Tire Test Rig and Vehicle Roll-Over Stability Control

Derek Martin Fox

Thesis submitted to the faculty of the Virginia Polytechnic Institute and State University
in partial fulfillment of the requirements for the degree of

Master of Science
In
Mechanical Engineering

Approved
Saied Taheri, Chair
John B. Ferris

Disapproved
Mehdi Ahmadian

Presented on December 9, 2009
Danville, VA
Keywords: Portable Tire Test Rig, Vehicle Rollover Mitigation Techniques

Design of a Portable Tire Test Rig and Vehicle Roll-Over Stability Control

Derek Martin Fox

Abstract

Vehicle modeling and simulation have fast become the easiest and cheapest method for vehicle testing. No longer do multiple, intensive, physical tests need be performed to analyze the performance parameters that one wishes to validate. One component of the vehicle simulation that is crucial to the correctness of the result is the tire. Simulations that are run by a computer can be run many times faster than a real test could be performed, so the cost and complexity of the testing is reduced. A computer simulation is also less likely to have human errors introduced with the caveat that the data input into the model and simulation is accurate, or as accurate as one would like their results to be. Simulation can lead to real tests, or back up tests already performed. The repeatability of testing is a non-issue as well.

Tire models are the groundwork for vehicle simulations and accurate results cannot be conceived without an accurate model. The reason is that all of the forces transmitted to and from the vehicle to the ground must occur at the tire contact patches. This presents the problem of obtaining a tire model. Tire companies do not readily give out tire data since the tire industry is still as much “black art” as it is science. For tire data one must begin with a testing apparatus. The test rig must be accurate and must have been validated before results can be used.

This thesis presents the process of the design and construction of a portable tire test rig. It then will discuss tire testing procedures and validation techniques. The resulting data shows good correlation between test data and known tire test data from flat track testing provided by a tire manufacturer. Then, a simple rollover study of a military truck will be compiled in TruckSim. Lastly, a control method for the rollover case will be designed and implemented. The results of the roll control simulation are positive. The study shows an increase in dynamic roll stability due to the implementation of the control algorithm.

Dedication

I would like to dedicate this effort to those who supported me and gave me hope through this experience; my wife Dana, my parents and other family, the other graduate students in Danville who became my good friends, the companies at VIR and their staff for keeping me entertained, and my other friends and coworkers who gave me support. I really do appreciate it. All of these people have taught me a lot, and have helped me become the person I am, and want to be. I would also like to thank God for helping me through every part of my life, possibly the only one who has never lost faith in me. I am so grateful to all of these people and I hope that I can repay the favors I have received in some fashion.

Acknowledgements

I would like to acknowledge TACOM for sponsoring and funding this project. Special thanks are due to Dr. Alex Reid for serving as the technical monitor for the project. Without the support of the military this project would not have been possible. Views expressed in this thesis are those of the author, and not the U.S. Army.

Contents

List of Figures

List of Tables

1. Introduction

Tire testing has traditionally been performed on flat track machines. These machines are large, belted surfaces that accept a rolling tire and resultant force and moment data is taken through a range of slip angles and/or camber angles. There are very few portable tire test rigs in operation, but the advantages are that they can be driven on real road surfaces instead of a simulated rolling road belt. The disadvantages are some increased complexity, and a greater need to keep the tests consistent.

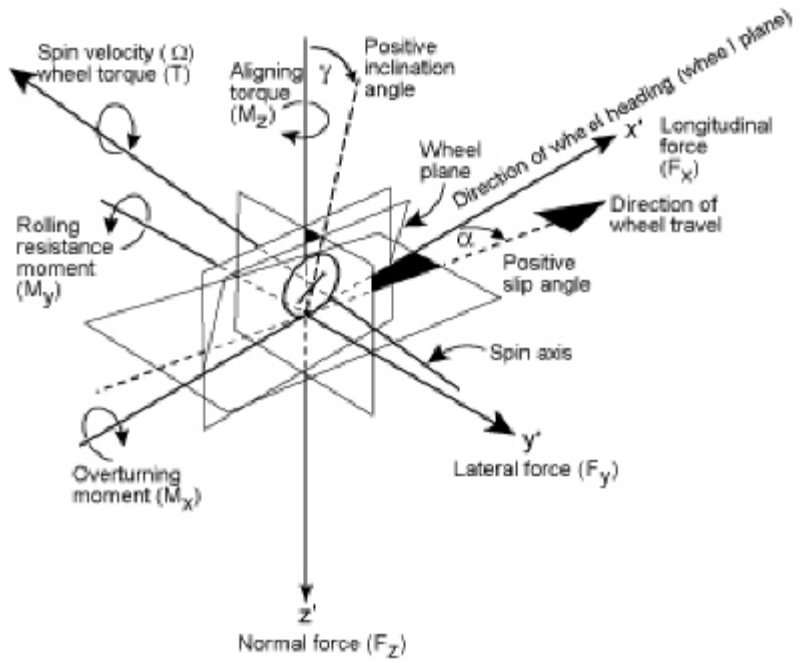

Figure 1. SAE Tire Coordinate System [1].
(Reprinted with permission from SAE J670e © 1976 SAE International. Further use of this figure is not permitted without permission from SAE.)

A good tire dataset will consist of 3 forces, Fx, Fy, Fz and 3 moments Mx, My, Mz, as shown in Figure 1, about the tire contact patch for a range of slip angles and camber angles and at multiple different loads and pressures that the tire may see in operation.

A tire model, such as the Pacejka Magic Formula [2] can take this tire data and characterize it based on its values. This type of model is a semi-empirical model and is the most popular method to model tire behavior. The Magic Formula model is well known for being robust and accurate for a multitude of tires and is used throughout academia and industry as a standard measure of tire performance. It is comprised of roughly twenty coefficients, formula version dependent, that are used in a handful of formulas to calculate tire forces.

Vehicle simulations are very useful tools for testing various parameters that affect, or are affected by vehicle performance. The range of possibilities is infinite and just as complex so many times assumptions must be made in order to take full advantage of the cost and time benefits that simulation offers. Judgment calls must therefore be made and a realistic view of the project must be understood for any improvement to be made. There may be no use spending 90% of the time allotted for the project to gain the remaining 10% of accuracy that the simulation can give. On the other hand, these results may be of use for those looking to find the last bit of performance. Simulation is a game of diminishing returns and compromises. The influence of the tire force capabilities on vehicle handling is so great that measured tire data, or a good tire model, is a necessity when doing vehicle simulations.

1.1 Motivation

The rollover mechanisms for vehicles in general are categorized as tripped or un-tripped. In situations where un-tripped rollovers occur, the tire plays a fundamental role. In order to study rollover through modeling and simulation, tire data was needed on various surfaces. Although it is possible to acquire data from various testing facilities, the data is limited to a single road friction coefficient. More tire data is needed in order to study the vehicle rollover behavior on various road surfaces. The motivation for this project was to develop a user-friendly, relatively low cost, repeatable, and easily accessible portable tire testing rig for collecting data on various road surfaces. This rig would demonstrate value further by allowing for wet tire testing and capability for testing on non-paved surfaces. TACOM, the project sponsor, also had the need for vehicle

rollover research. A mechanism that would aid in heavy vehicle rollover situation was also designed and studied.

1.2 Approach

The approach for the project was a straightforward design cycle from conception to fabrication, completion, and validation. Tire testing and simulation model tuning were then completed. The following list of tasks is a summary of what was accomplished. The design and construction of the rig took approximately one year to complete. Then the controller design for the rollover study was carried out in parallel with the rig construction. Lastly, tire testing was undertaken for rig result validation.

1.3 Thesis Outline

This thesis demonstrates the development of a portable tire testing rig and its capabilities. Chapter 2 introduces the design, construction, recommendations for, and future modifications of the rig. It also illustrates its performance specifications. Chapter 3 explains the methods and uses for tire testing with the rig. Testing procedures, validation runs, data collection, and signal processing. Test data will then be compared to known data for similar tire profiles in order to validate the testing. Chapter 4 illustrates simulation techniques with TruckSim. Chapter 5 shows the architecture of the rollover mitigation strategy as well as evaluation of the control algorithm. Rollover criterion is also presented in this Chapter. Chapter 6 concludes the study and suggests future work for the test trailer.

This thesis demonstrates the development of a portable tire testing rig and its capabilities. Chapter 2 introduces the design, construction, recommendations for, and future modifications of the rig. It also illustrates its performance specifications. Chapter 3 explains the methods and uses for tire testing with the rig. Testing procedures, validation runs, data collection, and signal processing. Test data will then be compared to known

data for similar tire profiles in order to validate the testing. Chapter 4 illustrates simulation techniques with TruckSim. Chapter 5 shows the architecture of the rollover mitigation strategy as well as evaluation of the control algorithm. Rollover criterion is also presented in this Chapter. Chapter 6 concludes the study and suggests future work for the test trailer.

2. Tire Test Trailer Design and Construction

2.1 Introduction

Tire force and moment data is needed by an engineer to conduct accurate vehicle dynamic simulations. Many simulations are carried out without this data and use generalized tire models which do not provide the accuracy needed for a good model. More information is better in this case as it gives the engineer a more complete model. The tire test rig presented in this thesis allows for a model as complete as necessary by its flexible design and construction. Virtually any on-surface test can be performed with the apparatus so the tire model is then as complete as real testing can allow.

This Chapter steps through the design and construction of a portable tire test trailer. Design considerations and decisions are presented about all components and subsystems of the trailer. First, the tow vehicle and trailer selection are discussed. Second, the structure of the rig and main components are shown. Next, the control station is presented. Last, the accessories of the design are given and future work is suggested.

2.2 Background

The IMMA group of the Department of Mechanical Engineering, University of Ma´laga Spain [3] is one such group who has conceived a flat track tire testing machine. This rig has capabilities for drum testing and flat track testing, a benefit for greater versatility. The rig results are the 3 forces and 3 moments about the tire contact patch as well as the slip and camber angles involved. The tire can be loaded vertically by differing amounts, a standard feature on tire test rigs. MTS is a manufacturer of tire testing rigs and is known to be one of the largest suppliers throughout the world [4]. Their machines use a flat stainless steel belt as the road surface [5]. Although very repeatable, in my opinion

these machines can give results that are not directly comparable to real road surfaces in terms of the means with which tire forces are generated. None-the-less these machines are useful for comparison purposes between tests made on the same machine.

The Laboratory of Automotive Engineering at Helsinki University of Technology has designed and developed a tire testing trailer for measuring longitudinal forces [6]. Their machine was designed mainly for testing tire friction on icy road conditions. It can develop slip ratios between 0 and 100 percent. They generally test at 10, 30, and 50 kph for consistency and can handle car wheels from 15 inches and up. Helsinki uses a two-tire trailer, one of which doubles as a trailer stability tire needed for operation, and also a lateral force balancing tire. A similar portable tire test rig for use with ice testing was also designed by Joakim Wennstrom of Lulea University of Technology in 2007 [7]. This design was for low loading conditions and slip ratio measurements only. An off-road tire testing apparatus was developed for testing agricultural tires in 1988 [8]. It too was created for longitudinal slip testing at varying static loads. The tire test trailer was not designed after any of these trailers, but knowing what a tire test rig could, and needed to, accomplish was the basis for the design.

Lateral tire testing is also very important when using tire data in a vehicle dynamic simulation. Phettplace, Shoop, and Slagle have completed testing of such lateral forces on off-road terrains [9]. Namely on variants of snowy surfaces, these measurements were carried out under approval from the U.S. Army. The need for off-road tire testing is present and was a driving factor in the conception of this thesis' work. Tests have yet to be conducted on surfaces other than asphalt because that was not within the scope of this project. The Idea is the same however, in that empirical data is gathered on alternate surfaces and can be used alone, or through a Pacejka model, in vehicle simulations for more accurate results on alternate road surfaces.

The Dunlop aviation tire group faced loading challenges similar to those that were encountered during this design project [10]. High load values and a means to apply them led Dunlop engineers to electro-hydraulic loading of their tire test rig. The dynamometer used in that rig also is similar in concept to the force hub used in this project. Many other research-based tire test rigs have been designed and built, but the tire industry is still a secretive entity so data on the commercial units are difficult to come by.

Tire models are as important as tire data for vehicle simulations. They are used to characterize tire forces and moments and can generalize tire performance. The tire model is the device that translates tire data into a working interface for the simulation software. The tire test trailer gathers empirical data that can be used alone, or with a semi-empirical tire model. Purely analytical models exist but are outside the scope of this thesis. A brief description is provided here however. Lugner, Pacejka, and Plochl describe the most recent and most used tire models in industry [11]. These range from frequency based models to handling type models. Salaani presents a tire model that calculates tire forces and moments using physical parameters of tires [12]. This method is analytical and worth mentioning. It is derived from classical mechanics and friction theory. Tire design is important to this method of modeling, so fundamental mechanics may not correlate with reality exactly. E.R. Gardner gives a brief background on tire design [13].

2.3 Tire Test Trailer

The tire test trailer (TTT) presented here is comprised of 6 major sub-systems. The load frame contains and locates most of the other sub-systems inside of the trailer, the force hub gathers the force and moment data, the steering mechanism develops the slip angles used for the tests, the loading mechanism adds and removes load to the tested tire, the data acquisition and control algorithms store data and control the sensors and actuators during the tests, and the water spray system allows for wet-tire testing. Appendix B shows a compiled list of TTT capabilities.

2.3.1 Trailer and Tow Vehicle Selection

The donor trailer selection was based upon a large load limit capacity. A 28 ft. Pro-Line enclosed race car trailer was chosen because it met the design requirement of large loading capacities and is displayed in Figure 2. The trailer contains triple 7000 lb axles which more than exceed the design loading criteria. A pickup truck with a large towing capacity was also required to pull the trailer which could weigh in excess of 15,000 lb. A Ford dually was used for testing. A simple drawing of the planned load

distribution for the TTT is shown in Figure 3. The water ballast is stored inside the water tank, which lies on the trailer centerline, when high vertical load tests are desired. It should be noted that the water tank load would vary when wet testing, with a loss of weight as the run progressed. The CG of the trailer would shift rearward, but the load compensation on the test tire should compensate for lost water. This load transfer was not studied in this thesis since the water tank was kept empty for the duration of initial testing. This force is not included currently because testing shows that the trailer's weight can account for the current vertical tire loads.

Figure 2. TTT in Operation With Tow Truck Attached. [Photo by author 2009]

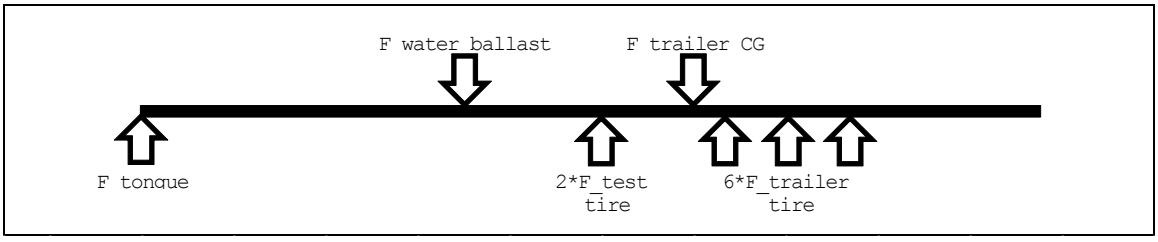

Figure 3. TTT Generalized Load distribution.

There is ample space inside for working and all components. At the front of the trailer is mounted the water tank and pump system. The load frame is position aft of the tank and all testing equipment is located inside of the frame. A Nitrogen cylinder is located next to the load frame for adjusting the pressure inside of the loading airbags. Aft

of the load frame is a work table where the electronic equipment is mounted. The placement of all components was mainly a function of packaging into the trailer design.

2.3.2 Frame Design

The frame for the TTT was designed to permit maximum space for testing equipment, good rigidity, and simplicity of construction. The frame was overdesigned by using some of the strongest, heaviest, and most workable material available to me. Weight was not an issue for the frame design because trailer lift could occur when the test tire was loaded. The weight of the frame assists in this matter. Additional ballast is also available by means of the water tank, but testing with loads high enough to permit this has not been carried out or needed yet. The large area needed for the test bed was fit in front of the triple axles so that the lifting effect onto the tow truck tongue could be more easily balanced with the ballast.

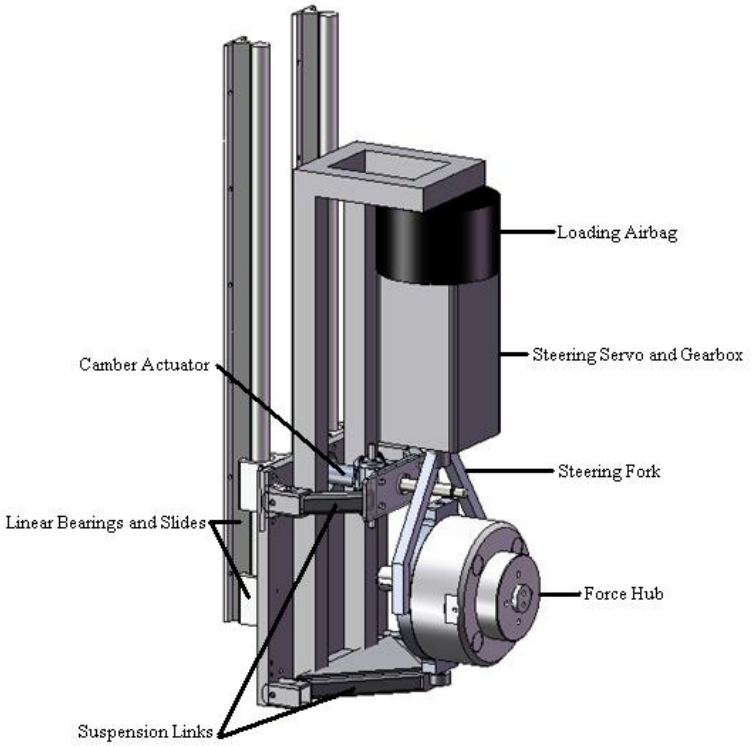

Figure 4. Solidworks Model of Tire Testing Subassemblies.

The stock trailer chassis was constructed from 6 in. x 2 in. -1/8 in. wall c-channel 1020 steel. This material is adequate for vertical loads that a trailer would see when used as it was designed, but was not a suitable platform for the TTT. A perfectly rigid structure would be ideal and it was visually seen that the stock trailer frame flexed when one side was jacked up. Reinforcement was needed so the lower portion (base square) of the TTT frame was designed and fabricated from 6 in. x 2 in.-1/4 in. 1020 steel. The upper TTT frame was fabricated from 4 in.x2 in. 1020 steel rectangular tubing. Lighter, thinner material was available, but additional weight over the test bed is actually beneficial. Vertical and horizontal members were constructed from ¼ in. wall tubing and the supporting triangulating members were constructed from 1/8 in. wall tubing. All welding was carried out by myself and post weld visual checks were done for verification.

The dimensions chosen for the frame were based on inside dimensions of the donor trailer and were maximized to allow for all components and test tires sizes. CAD drawings are shown in Appendix C. The two vertical members on either side of the frame above and below the base square contain linear bearing slides for the TTT fixture plate, which is discussed in Chapter 2.3.6.

An FEA study was performed on the TTT load frame to validate the design. The desired tire testing load of 5 kN (1124 lbf) was applied vertically up to the frame at the mounting for the slide rails on one side of the frame. The frame base was constrained to simulate it being welded into the trailer. The results are shown in Figures 5 and 6. The maximum displacement shown is about 0.001 in. and the factor of safety given for the frame is 171.

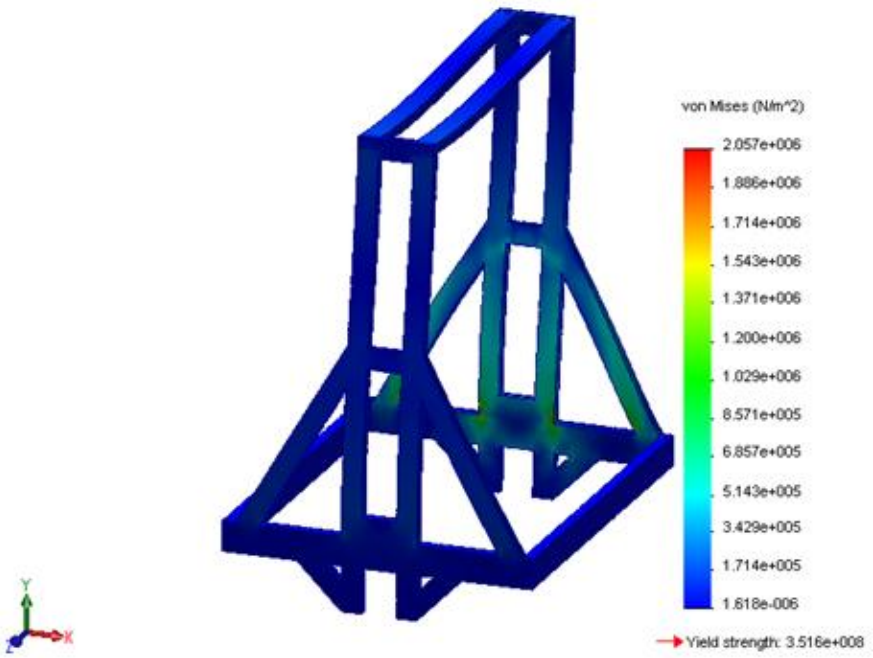

Figure 5. Load Frame FEA Displaying Stress Distribution.

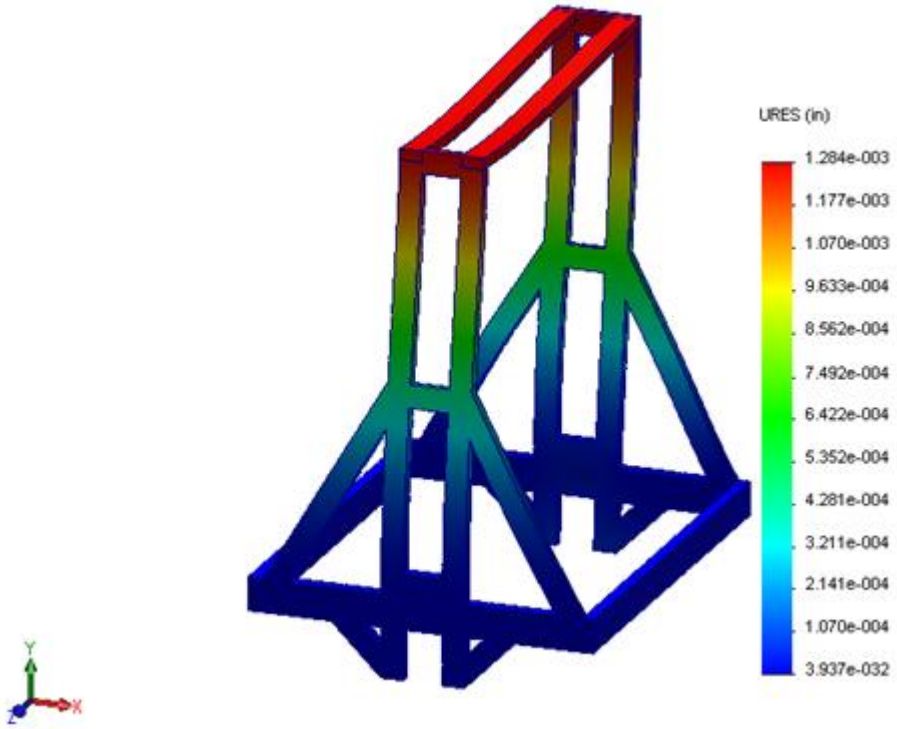

Figure 6. Load Frame FEA Displaying Displacement Distribution.

All welding on the trailer components was visually inspected for amount of penetration. Shigley gives a value of 0.3*Tensile Strength of the base metal for shear

loading applications [14]. Assuming 60,000 psi as the tensile strength of 1020 steel, 1/8 in. weld thickness, 149 inches of weld per side of the frame per Appendix C, a maximum vertical load of 1125lbf (5kN) based on one loaded tire, even loading, and a safety factor of 10 we see that the welding of the frame is adequate for these test conditions.

$$\sigma = \frac{F}{A} = \frac{1125*10}{0.125*149} = 604\ psi \quad (1)$$

The stress on the welds of the frame is far less than the allowed 18,000 psi per Shigley.

Limitations to the TTT frame design could be a natural frequency that is not high enough to mitigate noise from tire testing. The addition of the frame into the stock trailer has increased the trailer's frequency, but it is not currently known if this amount of stiffening is high enough. The frame is known to be stiffer due to the quantity and means of reinforcement to accept loading caused by tire testing. Another crude experiment was carried out by jacking one side of the trailer and observing flex. It was noticeably less than the prior test at stock condition.

2.3.3 Force Hub

A force hub is a measurement system comprised of multiple sensors that have the capability to measure many forces and moments acting on the tire. Sometimes called force transducers, these units are necessary to a tire test rig so the force and moment data can be collected. Other methods exist for collecting this data, such as strain gauge instrumented suspension link systems, but are complex and difficult to obtain accurate data from. The force hub allows everything needed to be contained in one package which greatly simplifies the testing. Two main types of force hubs exist and consist of the strain gauge type and the piezoelectric type. The latter was chosen for this project.

The force hub that was chosen for this TTT design was a Kistler RoaDyn® P530 measuring hub. The hub measures forces and moments about all three axes: $F_x, F_y, F_z, M_x, M_y, M_z$. It uses a supplied amplifier to send these signals to the DAQ system. This system is discussed further in Chapter 3.2. It contains four, 3-component force sensors that are preloaded between the base and top plates. This method allows for a very high natural frequency of the system, and low interference among the signals from

the 4 sensors. An oiling system inside of the unit protects it from overheating, and undue wear. The unit is completely sealed and designed for use in weathered environments also, so water, ice, and off-road testing do not present a problem. Provisions for a braking or torque system are also given on the back side of the unit in the form of a keyed shaft that can accept a brake rotor or engine shaft coupling [15].

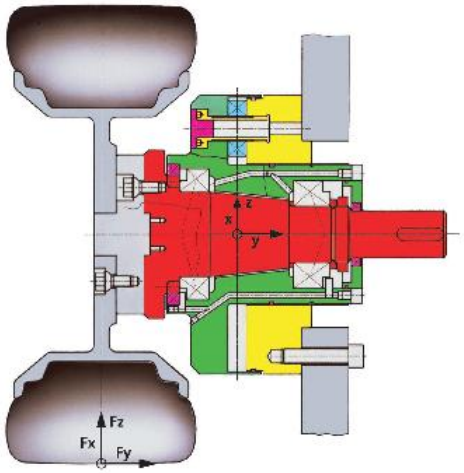

Figure 7. Cross Section of Kistler Force Hub [16].

This specific hub was chosen for the specifications and wide range of use that the unit encompasses. It is an easy to integrate unit that was the proper size to mount into the TTT. The mounting system of the hub also matched the design of the suspension system chosen for the TTT. It is capable of holding wheels over 13 in. and different wheel bolt patterns can be utilized if adapter hubs are used. Its 6744 lbf load capacity for vertical tire loading was also attractive and would meet the specifications for tires that would be tested. The sensitivity and hysteresis of the unit are also very small which would be beneficial for testing accuracy and repeatability. A complete specification sheet from Kistler which outlines the technical data for the hub is shown in Appendix A.

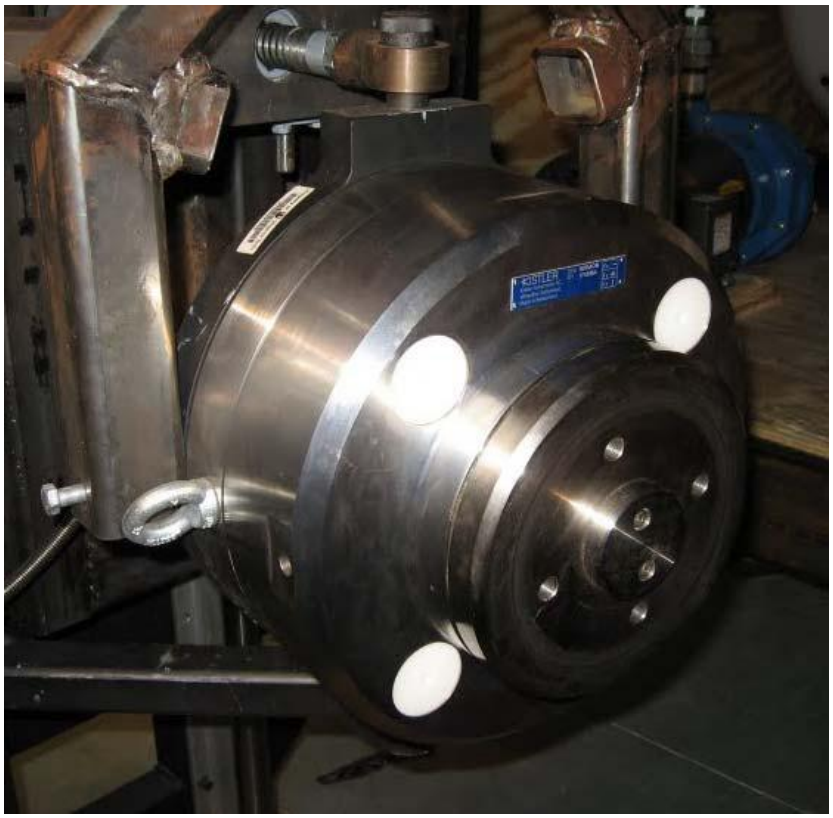

Figure 8. RoaDyn Kistler Force Hub Mounted in TTT. [Photo by author 2009]

2.3.4 Steering and Camber Mechanisms

The steering system was designed to fulfill the requirement for high resolution and accuracy of steering angle. The goal for steering resolution was a minimum 0.1 degree. This was chosen so that data could be captured at enough slip angle points during a test run. Similarly, the backlash goal of the system was chosen to be at maximum 15 arc minutes to minimize unwanted tire movement and vibration. This would be achieved with the backlash Figure of the entire unit. The design goal of steering angles was chosen to be -16 to +16 degrees. This was chosen since tire forces generally fall off before this value. The camber angle range was similarly chosen to be -10 to +10 degrees since tires are generally not operated past these points.

There are two main mechanical components to the steering mechanism. First, a Parker-Hannifin servo motor controls the actual steering. Second, a 153:1 Nabtesco inline gear head increases the torque and allows for much smaller increments of steering to be

applied to the wheel. The power system for this unit will be discussed further in Chapter 2.3.10.

Figure 9. Parker Hannifin Rotary Servo Motor Used for Steer and Camber Control [17].

The servo motor is a Parker Hannifin BE344-JJ rotary servo motor, displayed in Figure 9. It is coupled with a Parker S100V2F12I10T10M00 Servo Drive. The system was designed based on the given criteria, packaging, and a search through the manufacturer's catalog to match the desired specifications. This particular Servo motor was chosen to be compatible with a gear head reduction as shown below and to have a very small step value. It is a 2000L incremental encoder, so a resolution of the servo motor alone is 0.18 degrees. A design holding torque to combat tire self aligning moment of 300 ft-lb was used to size the steering servo motor and gear head ratio. This 300 ft-lb value was chosen based on a formula for normalized aligning moment given by Milliken [18].

$$M_Z = \bar{M}_Z * T_Z * \mu_Y * Z \tag{2}$$

A 0.5 maximum normalized aligning moment, $\bar{M}_Z$, was selected based on the given plot in the text. T_Z, the pneumatic trail was taken as 2.5 in. based on Wong's text [19]. μ_Y was chosen to be 0.9 and was also based on Wong. Road friction coefficient is discussed further in Chapter 3.3. The vertical load, Z, was chosen to be 1100 lbf (5 kN) since that was the maximum tested condition of the test tires. The resulting aligning moment was equal to 103 ft-lb. An additional safety factor of 3 was given to the design to obtain the 300 ft-lb desired torque value.

The Servo motor and gear head combination is compact and outputs sufficient torque for a steering during a tire test. The controllers for the steering motors are three phase 240V controllers provided by Parker. Specifications for this motor can be seen in Appendix A.

The gear head is a Nabtesco RD-040E-153 153:1 harmonic gearbox as shown in Figure 10. This unit was selected to be compatible with the servo motor and to provide a very large gear reduction. It does not introduce too much steering effort, and the backlash reduces the noise present. With this reduction in place, the resolution of the system is greatly increased, so the 0.18 degree Figure given from the servo motor becomes approximately 0.0012 degrees per step. This is far more precise than the design goal of 0.1 degrees, minimum needed for slip angle sweep testing. The gear head has less than 1 arc minute of backlash. It is an all inclusive package that is sealed and durable for easy maintenance. It is also relatively compact and has high torsional rigidity [20]. These features make the Nabtesco gear head a good fit for the TTT.

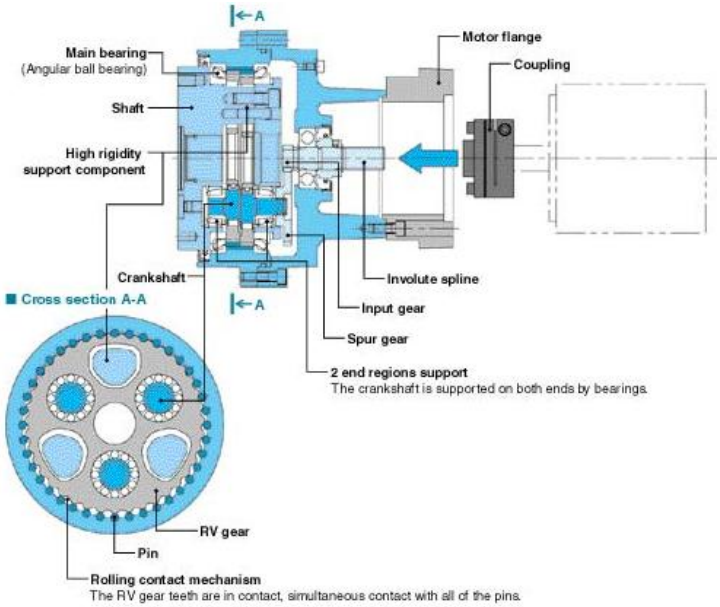

Figure 10. Nabtesco Cross Section Drawing of Inline Gear Head Used for the TTT [19].

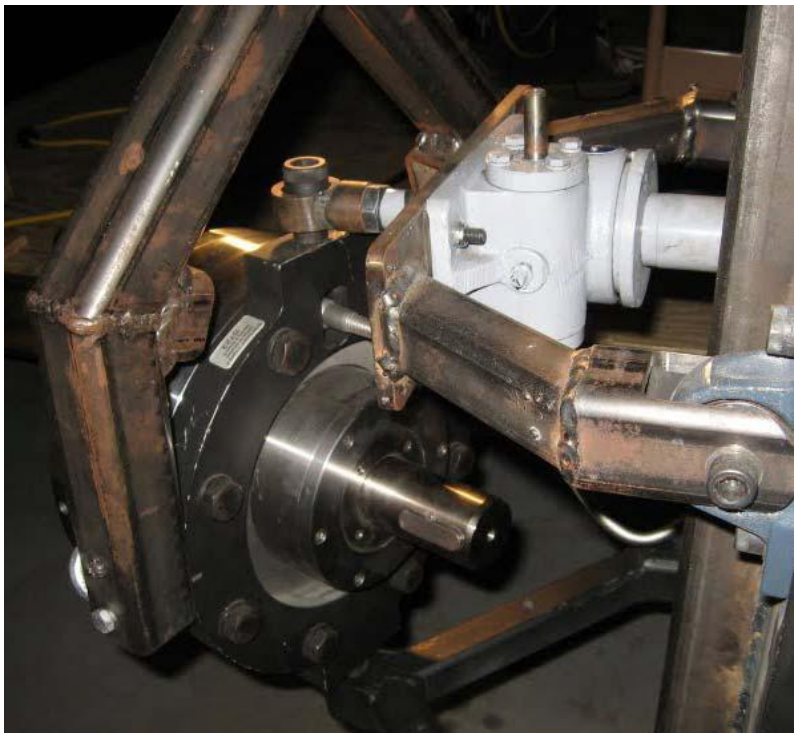

Figure 11. Steering Fork and Camber Mechanism During Fabrication. [Photo by author 2009]

The steering fork is used to transfer the rotation of the servo, post-gear head, to the tire and to transmit the vertical load to the hub. The vertical loading is discussed in Chapter 2.3.5. Detailed CAD drawings for the steering fork are given in Appendix C. The correlation after the gear head is a direct 1:1 so the angle of the steering fork is assumed equal to the tire slip angle. It is made from 1.5 in. 1020 steel square tubing with a ¼ in. wall. The kingpin axis was designed to be normal to the road surface so that no tire lifting would occur during the steering operation.

The steering fork was also analyzed in FEA to validate its design. A torque of 300 ft-lb was applied at the bolt mounting locations in the lower part of the fork. This value of torque was chosen based on tire aligning moment data as discussed in Chapter 2.3.4. The top face of the fork was constrained in all directions. The results are given in Figures 12 and 13. The maximum displacement of the fork legs is 0.036 in. and the strength factor of safety given for the entire design at 3 times the measured moment is 3.2. A simple compliance analysis of the FEA results at the design torque gives a variation of 0.29 degrees due to fork leg bending.

$$tan^{-1}\left(\frac{0.036}{7}\right) = 0.29\ degree \quad (3)$$

This value, plus the backlash figure of the gearhead gives a total maximum steering system compliance of 0.3 degrees. The effect of this fork twist on test data is discussed in Chapter 3.3. Steering kinematics are also discussed later along with suspension design.

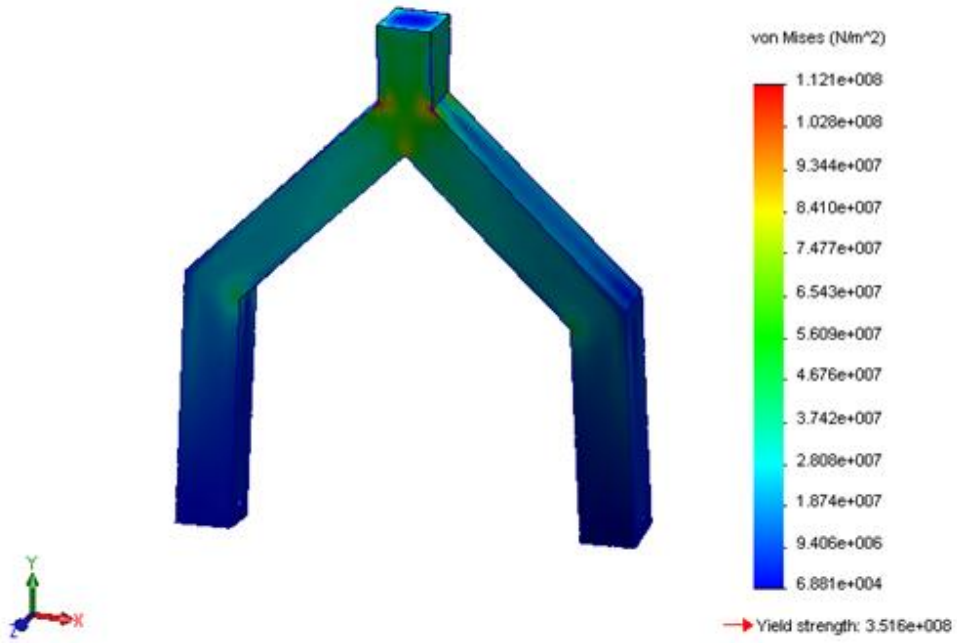

Figure 12. Steering Fork FEA Displaying Stress Distribution.

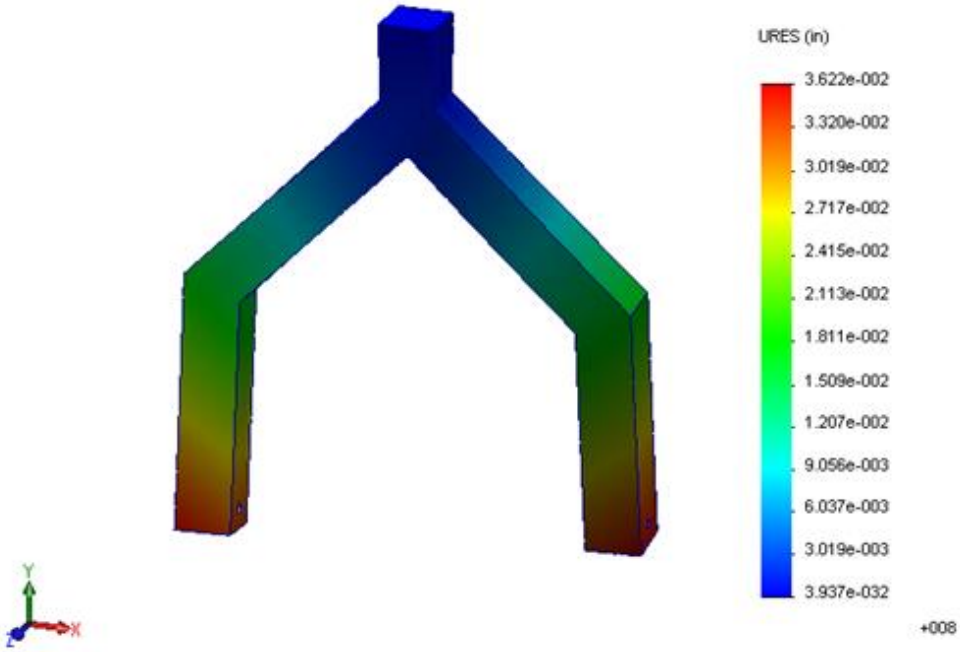

Figure 13. Steering Fork FEA Displaying Displacement Distribution.

The force hub is mounted to parallel, equal-length, double wishbone type suspension links. Milliken gives detailed background on the design of various independent suspension types [17]. This type of suspension was chosen for ease of fabrication and packaging. It adds minimum complexity since double wishbones constrain five of the six necessary degrees of freedom. The steering fork and motor constrain and control the sixth. Parallel links were designed into the system so that no camber change would occur when the unit was raised or lowered for varying tire sizes. The links should be positioned parallel to the ground for testing. They are made from 1.5 in. square 1020 steel tubing with a ¼ in. wall. 2-D suspension kinematic analysis was completed and is displayed in Figure 13. It is seen that no camber change occurs due to the parallelogram formed by the suspension links in the front view.

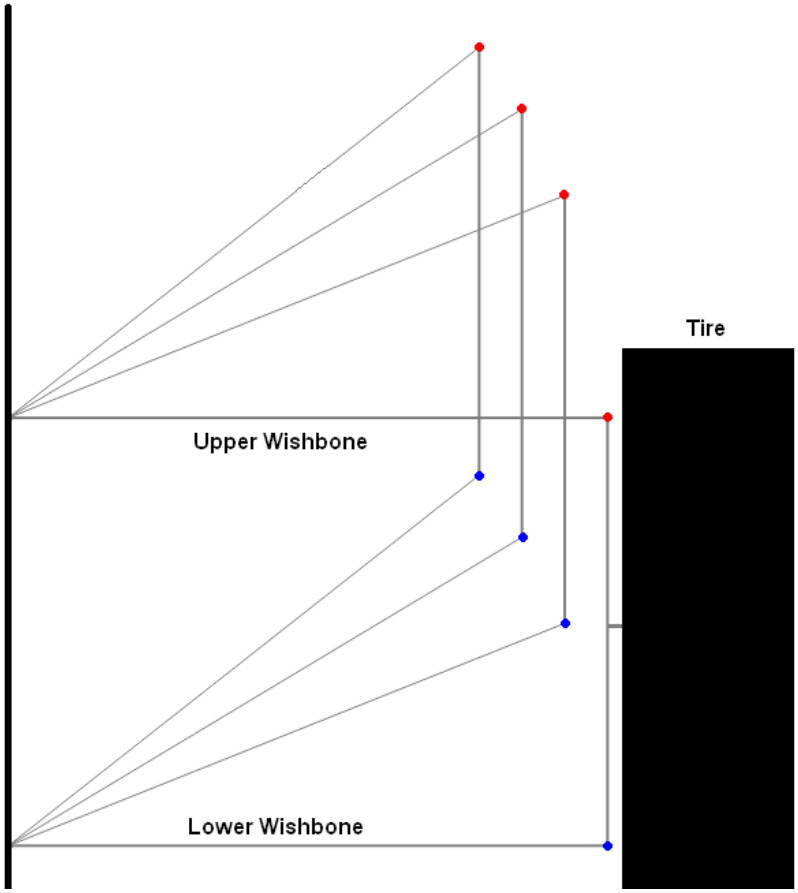

Figure 14. 2-D Suspension Kinematic Analysis.

This design helps to eliminates additional setup time. The Equal length members were designed so that there would be no initial camber. Camber is controlled by the small mechanical screw actuator as shown in Figure 14. Both of these geometry features also contribute to zero camber change if minor displacement variations occur during a run. These variations should be controlled by the load compensating regulator, but this adds an additional safety factor against unwanted results. Run setup is discussed in Chapter 3.2.

The suspension links were designed with zero caster so that no tire lift or camber change would occur with steering. This would adversely affect test results. This is also beneficial because it eliminates mechanical trail from the system which would alter aligning moment data.

A simple calculation for loading was made for the suspension links. The included angle of the link members is 90 degrees. Detailed drawings are given in Appendix C. A side load of 2000 lbf was selected based on the Pacejka magic formula applied to the known coefficients of the tires to be tested. The area of the tube is A.The applied force into the link is F. Assuming a Yield Strength of 30000 psi and comparing this with calculated stress it can be seen that the links are strong enough for this force level in compression.

$$\sigma = \frac{F}{A} = \frac{2000\ lbf * \sin(45)}{1.25\ in^2} = 1130\ psi \qquad (4)$$

Figure 15. Steering Fork and Camber Mechanism Completed. [Photo by author 2009]

2.3.5 Loading Mechanism

The tire loading mechanism was designed to be simple and robust. A maximum load of 8000 lbf was chosen based on the maximum load capacity of the largest tire to be tested. The loading mechanism also needed to have a wide range of available force, and must be able to withstand some horizontal loading. Screw actuators were researched but sufficient means of load adjustment would add too much cost to the project. An air spring was chosen for these reasons as it would best fit the design criteria. A Firestone double-convoluted 20-2 air spring was selected for the load mechanism. It is 12 in. in diameter and has an installed height of 5 in. It can produce a maximum load of 8630 lbf at the installed height and 100 PSIG. This load is greater than the force hub can handle so is not the limiting factor in the loading system. Nitrogen pressure controls the load and is monitored by the electronic pressure regulator discussed later. Hydraulic ram loading was considered but not chosen based on additional complexity as well as based on private conversations with a field expert. Hydraulic loading was thought to have the possibility of additional system noise [21].

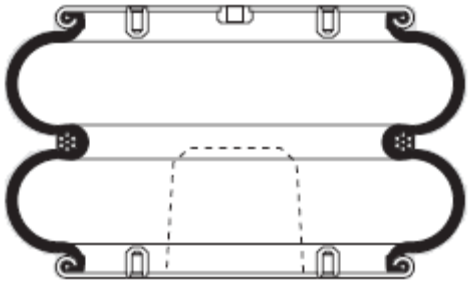

Figure 16. Cross Section of Firestone Convoluted Airbag Used for the TTT [22].

The convolution, as seen in Figure 13, provides more lateral rigidity which is needed when the test wheel is cambered. The specification sheet from Firestone Industrial is given in Appendix A.

The load is transmitted to the hub through a miniature load frame which is mounted to the gearbox. This is shown in Figure 14 and was needed because load could not be applied directly to the top of the servo motor. The load then travels through the steering fork and into the hub which measures and records it. The forces on the steering

fork would not vary by terrain because the trailer was designed for flat ground testing. However, small vertical force variations on any terrain can be dealt with by the load compensation discussed below.

Figure 17. Pneumatic Regulator Mounted in TTT. [Photo by author 2009]

An electronic pneumatic regulator was chosen to control the pressure in the air spring. It has a blow-off valve to decrease pressure if it is too high. The regulator was connected to a Nitrogen tank and to the air spring, and is controlled via a LabView controller to monitor and add pressure as needed during a test run. The LabView controller was developed by a third party so further details are not included here. Nitrogen was chosen since it is easily obtained from local supply stores in a tank, so that an air compressor is not needed. It is also less affected by temperature so that does not need to be taken into account.

2.3.6 Component Mounting Fixture

The TTT component mounting fixture was designed to locate all necessary components required and to remain rigid during testing. It was constructed from 1 in. 1020 steel plate and was CNC cut and drilled for accuracy. All bolt holes are tapped UNF thread for quick assembly, and to negate the use of nuts for packaging reasons on the rear. The plate locates the suspension links, the tire loading and steering frame, and the

linear bearings. The entire unit is raised and lowered by a 2 ton mechanical screw actuator and is used to change height based on tire size as well as for storing the test tire off the ground for transportation. The TTT can accommodate tire sized from 23 in. to 38 in. This screw actuator is shown between the linear bearing slides in Figure 14.

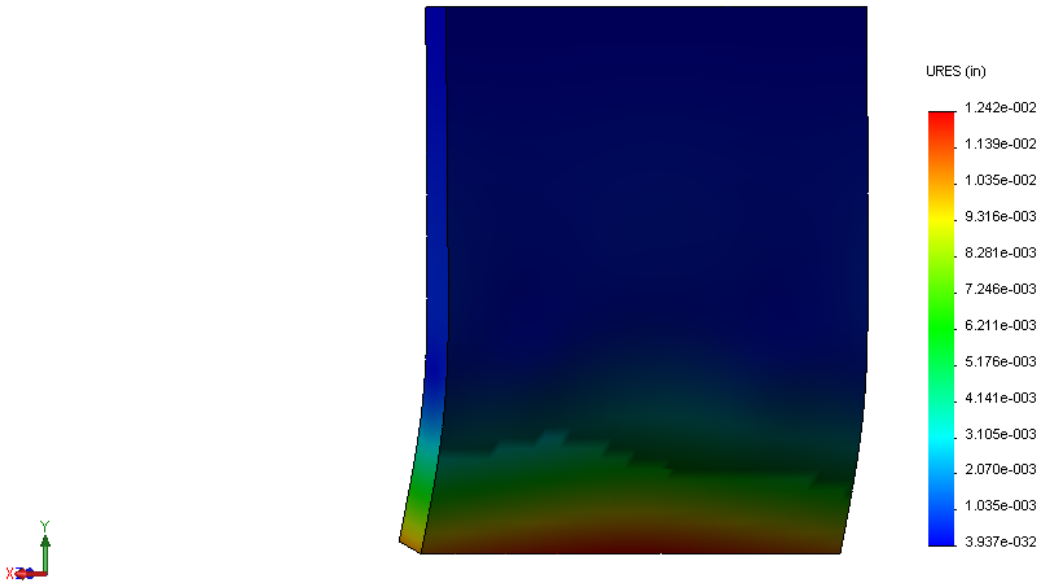

Figure 18. Mounting Plate FEA Displaying Displacement Distribution.

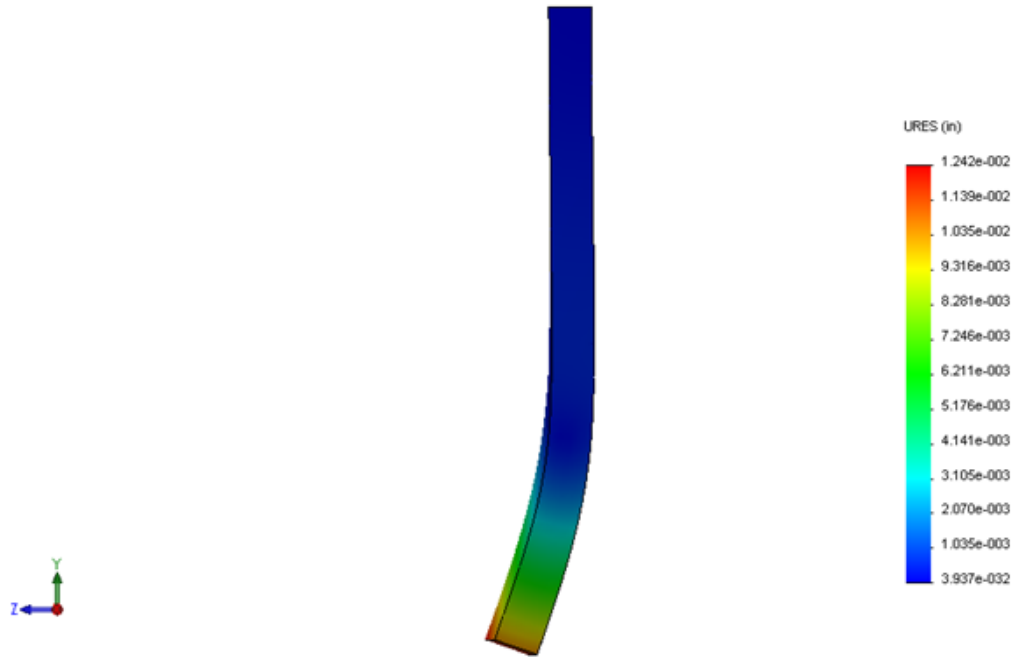

Figure 19. Mounting Plate FEA Displaying Displacement Distribution (Side View).

The FEA performed on the mounting fixture is shown in Figures 18 and 19. The plate was constrained at the linear bearing block mounting locations and a 2000 lbf load was applied to the lower suspension mounting location. This load was taken from the Pacejka model of the tires to be tested and is representative of the maximum lateral force capability of those tires. The FEA was based on a worst case scenario where all force was transmitted through the lower link. This was done because the plate is cantilevered over the linear bearing blocks.

Figure 20. TTT Sliding Mounting Fixture With All Components Attached. [Photo by author 2009]

The linear bearings used were Teflon-lined, self-aligning bearings that were chosen to reduce friction in the slider mechanism. They were sourced from LM76 due to their self-lubricating nature and all-weather capabilities.

Figure 21. Component Mounting Fixture Backside With Linear Bearings. [Photo by author 2009]

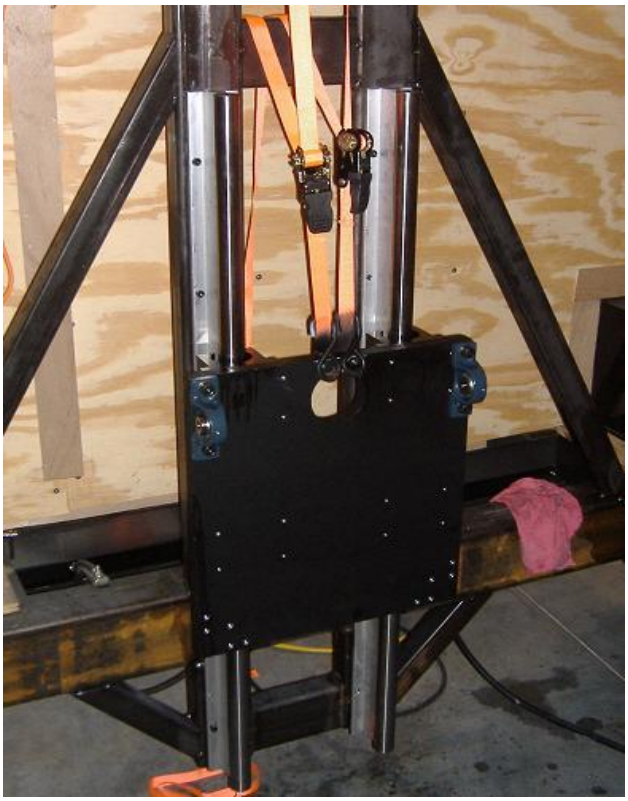

Figure 22. Component Mounting Fixture Mounted on Load Frame. [Photo by author 2009]

2.3.7 Parallel “Dummy” Tire

The TTT design is made to allow a second tire to be mounted on the opposite side of the trailer to run in parallel with the test tire. It would be setup with the same tire, loaded the same, and steered in the opposite direction as the test tire. This tire is not designed for use with a force hub, but utilizes all of the other same components that the test tire uses. It was designed into the system in order to balance the yaw moment induced on the trailer during a test run. This yaw moment could tend to increase the trailer yaw angle, thereby altering the tire’s slip angle artificially. The loading of this tire would also balance the forces about the X axis which currently could steer the trailer by unloading one side of trailer tires, causing the opposite to carry more load. Any lateral force then produced by the trailer tires would be amplified since one set would be operating at a much higher load. This would unbalance the yaw moment on the trailer and change the test tire slip angle as well. The negative aspect of the dummy tire is that there is more induced drag caused by tire slip and it would be more difficult to maintain a constant speed. As it is now, one tire permits enough drag to cause a need for the truck driver to essentially learn the speed loss and account for that with throttle inputs. The capability for adding a dummy tire is present but has not been implemented yet because validation testing for the rig needed to be completed before moving further into the project.

2.3.8 Data Acquisition System and Control Algorithm

The data acquisition board used for the TTT was selected to be an NI USB 6212. It is a relatively simple USB connected data board that has both analog and digital inputs. The original design incorporated linear potentiometers to measure camber angle by measuring effective length of the upper wishbone but is not currently being used. Camber is currently measured by taking the angle of the wheel face with the road. The DAQ board was chosen to be able to connect to this sensor and the servo controllers. The setup of the DAQ board, the LabView based GUI and control algorithm was implemented by third party. Its structure and design are outside the scope of this thesis. Figure 19 is the

main page for this GUI. The design is simple and easy to operate. The user needs to first define the sweep frequency and maximum slip angles and the program then steers the tire through one complete slip angle cycle in a sine wave format. The output data is then stored on the desktop in a specified folder. This program was used to capture all test data presented here. A stop all button is located in the trailer in case of an emergency.

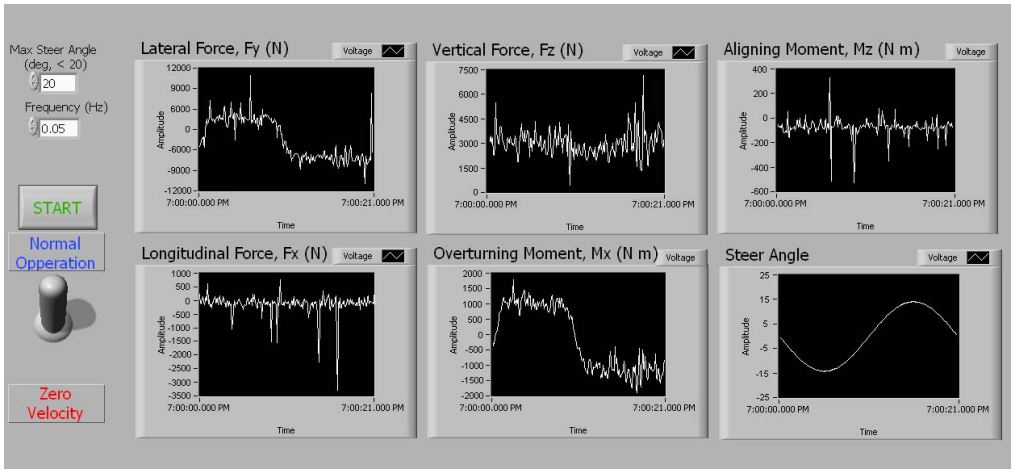

Figure 23. LabView Data Collection Program Main Page.

2.3.9 Water Spray System

The water spray system will be used during wet testing runs by spraying water ahead of the test tire, thus creating a simulated wet-road condition. The system is composed of a 500 gallon water storage tank, a Goulds water pump, and the necessary plumbing lines and fittings.

Figure 24. Goulds Pump Mounted in the Front of TTT. [Photo by author 2009]

The water pump chosen was a Goulds brand impeller pump and is shown in Figure 24 in its final mounting location. It is powered by a standard 110V outlet, so it is easily powered in the TTT by the generator. The pump output curve is shown in Appendix A. Water flow rate needed was calculated based on depth of water desired, width of water desired, desired pump efficiency of 72%, and a test speed of 30 mph. A spreadsheet showing flow rates, water widths, water heights, and available test speeds is also shown in Appendix A. The maximum water depth for a 30 mph test run is 10mm.

Figure 25. 500 Gallon Water Storage Tank Used for Wet Tire Testing [23].

Figure 25 shows the chosen 500 gallon water tank that is mounted at the front of the trailer to store enough water for about 3 test runs at the maximum water depth and width. The tank can also be used to provide up to 4200 lb. ballast with large vertical tire test loads.

Plumbing from the tank to the pump consists of 1-1/4 in. NPT fittings and stainless braided line. Another stainless line exits the pump and feeds a water distribution manifold with 6 incorporated nozzles (Mcmaster PN-3404K46). The nozzles are 30 degree flat spray pattern nozzles and are spaced so that even water coverage is given over 1 meter of width below the test tire. The nozzles are shown in Figure 26.

Figure 26. McMaster nozzles used in TTT spray system [24].

2.3.10 Power System

A Miller Bobcat 250 3-phase generator, as shown in Figure 27, was purchased to power the electricals inside of the trailer. Complete specifications for this unit are shown in Appendix A. This generator has ample power to run all components and electricals needed for test runs. Generator electrical noise is not considered since there is no other easy way to get this type of power to the trailer. The generator is mounted in the bed of the truck for safety reasons due to the emissions of the generator engine. Wiring is then sent rearwards to two breaker boxes mounted over the test table. One box is for 240V 3-phase power needed to drive the steering servos. The other box is 120V single-phase power used for everything else on the trailer.

Figure 27. Miller Bobcat 250 3-Phase Generator for On-Board Power of All Components [25].

2.4 Conclusions

In conclusion, I believe that the TTT design and construction is a very solid base for further testing and use since the data gathered during the validation experiments of Chapter 3.4 shows good correlation to known data. The TTT design is also robust enough to allow for more future modifications. The relative simplicity of the design also gives value to the TTT since repairs or changes would be easy to implement. Alternate surface testing should be carried out in the same fashion as on-road testing, and other types of tire models could then be developed. This rig opens up many new opportunities for tire engineers and adds integrity to vehicle simulations since actual tire forces and moment values can now be easily obtained. Relatively quickly setup and easily accessible, the TTT provides an accurate and repeatable method for collecting tire force and moment data. TTT setup and operation is discussed in Chapter 3.2.

Figure 28. Completed and Loaded Test Tire. [Photo by author 2009]

3. Tire Testing with Trailer

3.1 Introduction

The design of the TTT was based on the need for a simple, repetitive method for tire force and moment testing on a multitude of surfaces in the field. Repeatable data is given in Chapter 3.4. The trailer needed to be robust and easy to operate with two people. The TTT accomplishes these goals for testing as the test procedure is relatively simple.

After data is taken a complete tire dataset could be created. This would include camber values from at least 0 to 15 degrees in 0.5 degree increments, pressures plus or minus 10F of hot running pressure in two degree increments, and loads of one half to two times the rated load in roughly 100 pound increments.

The TTT can provide the following data; slip angle sweep data at discrete camber angles, lateral force and overturning moment versus camber angle, and lateral force and aligning torque versus slip angle. With the braking expansion planned it could also provide lateral force and longitudinal force versus slip ratio.

These curves are then implemented in a simulation program of the user's choice. This tire rig does not test for tire deflection, but that would need to be included in a tire dataset for use in simulation on off-road or bumpy terrains.

3.2 Tire Testing and Data Collection

The complete procedure for tire testing with the TTT is as follows: After arriving at a test site selected to have a suitably long, smooth road surface or off-road surface the user should power up the generator and the Labview GUI. The GUI automates the testing procedure so that nobody needs to be inside of the trailer for safety purposes. After initial checks, the load, tire pressure, maximum sweep angle, sweep frequency, camber, and road speed need to be selected. It is a good idea to have a test plan in order during this step. If camber other than zero is chosen, the desired value is attained by activating the camber servo and measuring the tire camber with a camber gauge. The users can then

begin the test by driving the test surface in a straight line and activating the system GUI when the test speed is achieved. The automated program then sweeps the tire slip angle to its extreme and then back to center. A stop all button is easily reached in the case of a failure. The GUI has then created a folder on the desktop of the user's computer with the run data inside. Tests are then repeated at different combinations of the selectable variables.

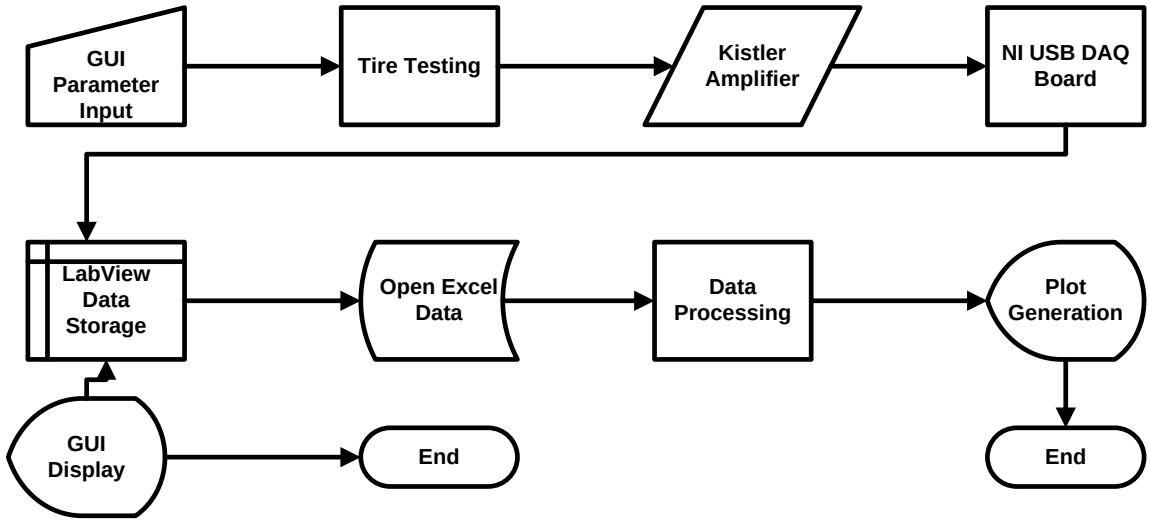

Figure 29. Flow of Data for a Test Run.

The set of collected test data for validation is shown in Table 1. This test set was made to validate the trailer's performance. Two different tires with known data were used to get a good comparison. The data from these two tires came from a third party source and the test conditions and tire makes and models were replicated for the TTT validation. The third party data was gathered on a flat track machine so data will be slightly different due to the coefficient of friction of the actual road surface used for the TTT test. Plotted data for this run log is given in section 3.4.

Table 1. TTT validation experiment. Gray runs are not plotted since Pacejka coefficients are known only at 50 kph.

Run	Tire	Speed (mph)	Load (N)	Sweep Max Angle (deg)	Sweep Freq (hz)	Slip Angle Speed (deg/s)
1	Goodyear Assurance TT 94T 215/60/16	10	3500N	15	0.05	SweepMaxAngle* sin(2*pi*SweepFreq*time)
2	Goodyear Assurance TT 94T 215/60/16	20	3500N	15	0.05	
3	Goodyear Assurance TT 94T 215/60/16	20	3500N	15	0.01	
4	Goodyear Assurance TT 94T 215/60/16	30	5000	15	0.01	
5	Goodyear Assurance TT 94T 215/60/16	30	5000	15	0.01	
6	Goodyear Assurance TT 94T 215/60/16	30	5000	15	0.01	
7	Goodyear Assurance TT 94T 215/60/16	30	5000	15	0.01	
1	Michelin Hydroedge 94T 215/60/16	30	5000	15	0.01	SweepMaxAngle* sin(2*pi*SweepFreq*time)
2	Michelin Hydroedge 94T 215/60/16	30	5000	15	0.01	
3	Michelin Hydroedge 94T 215/60/16	30	5000	15	0.01	
4	Michelin Hydroedge 94T 215/60/16	20	3500	15	0.01	

3.3 Signal Processing and Analysis

The data was processed after the entire dataset was collected. For these validation experiments, only lateral forces of the two tires were studied because they are the values most related to tire handling performance. Figures 30 through 37 are plots of the actual raw data (Tire Brand “Test), the fitted data (“Poly”), and the known data (Tire Brand “5kN”). The known data is the green line and was obtained from third party software that took in the known Pacejka coefficients of the test tires and created lateral force vs. slip angle curves. The Pacejka coefficients were known from the flat track testing. It is given to validate the TTT data.

Data is processed manually in Excel since it is fairly quick with a small amount of datasets. The data files were initially plotted and studied. The data needs to be clipped and the hysteresis loop averaged. After this, the data was re-plotted and a curve fitting routine was applied through excel's polynomial fit function.

The linear range of the data collected on the Goodyear tires shows slight discrepancies between given and TTT data. The lateral force is most notably recorded as lower from the TTT than is given. There is then a crossover around 6 degrees slip angle and the TTT records the lateral force as higher than the given data. Since the test road surface is likely a lower coefficient of friction than a flat track machine, this could be the reason for variances in the linear range of the tire. Wong gives values of 0.8-0.9 for road coefficients of friction [18]. These values vary with the condition and age of the road. It should be noted that the dip in lateral force on run 5 between 2 and 6 degrees slip angle was due to a quick acceleration of the test truck during the test run. The data begins to diverge around 10 degrees slip angle and then falls off, whereas the Pacejka fit data stays fairly constant over the range up to 16 degrees. Test run 6 shows the best correlation between the TTT and the given data because it does not drop off as early as the other runs.

It can be seen that the fitted TTT data follows the known tire data very well in the linear range of the Michelin tire. TTT data begins to diverge from the Pacejka fits a bit later than the Goodyear also. This divergence occurs at around 12 degrees slip angle compared to the 10 of the Goodyear tire. Test run 10 actually fits the given data very well up to the 16 degree maximum slip angle. The source of the divergence is due to the difference in testing methods (flat track and on road), and steering system compliance discussed earlier. Contributions from the non-present dummy tire, as discussed in Chapter 2.3.7, could also be included but further testing would need to be completed.

Figures 38 through 40 are shown to demonstrate the repeatability of the TTT. The curve fit lines to the test data, shown in Figures 30 through 37, were extracted as is and plotted against each other for each tire tested. These plots are Figures 38 and 39. The minimum force value at each point was then subtracted from the maximum force value at each point. The resulting plot is given as Figure 40. The plot can be separated into two distinct sections. Low slip angle, 0 to 7 degrees, show low to medium amount of

variation between runs. This proves the repeatability of TTT data in the linear tire range. At higher slip angle, above 7 degrees, the repeatability begins to digress and differences between runs begin to show. This is most likely due to system total compliance, as its effects are unpredictable from run to run.

3.4 Sample Data

The following sample data was obtained from the TTT on a flat, straight, paved road surface, and with the water tank empty. This road was chosen since it was the closest surface available to compare with the known flat track data for the test tires. It was also easily accessible and had no traffic so it was a good place for testing with a large truck and trailer. It should be noted that the test road was slightly dusty during the test runs which could account for lower friction since flat track machines are kept clean and controlled. Ambient test temperature was 80 degrees Fahrenheit and road surface temperature was 110 degrees Fahrenheit. All tests were completed within two hours from the start and no weather change was noted.

3.4.1 Validation Experiment I

The first validation experiment for the TTT was performed with a set of Goodyear passenger tires. These tires were chosen because third party data was already known for the tires. Pacejka coefficients were also given with the known flat track data. Test run Figures begin at test run 4 because the previous three tests were used to shake down the rig and warm up the tires at lower speeds.

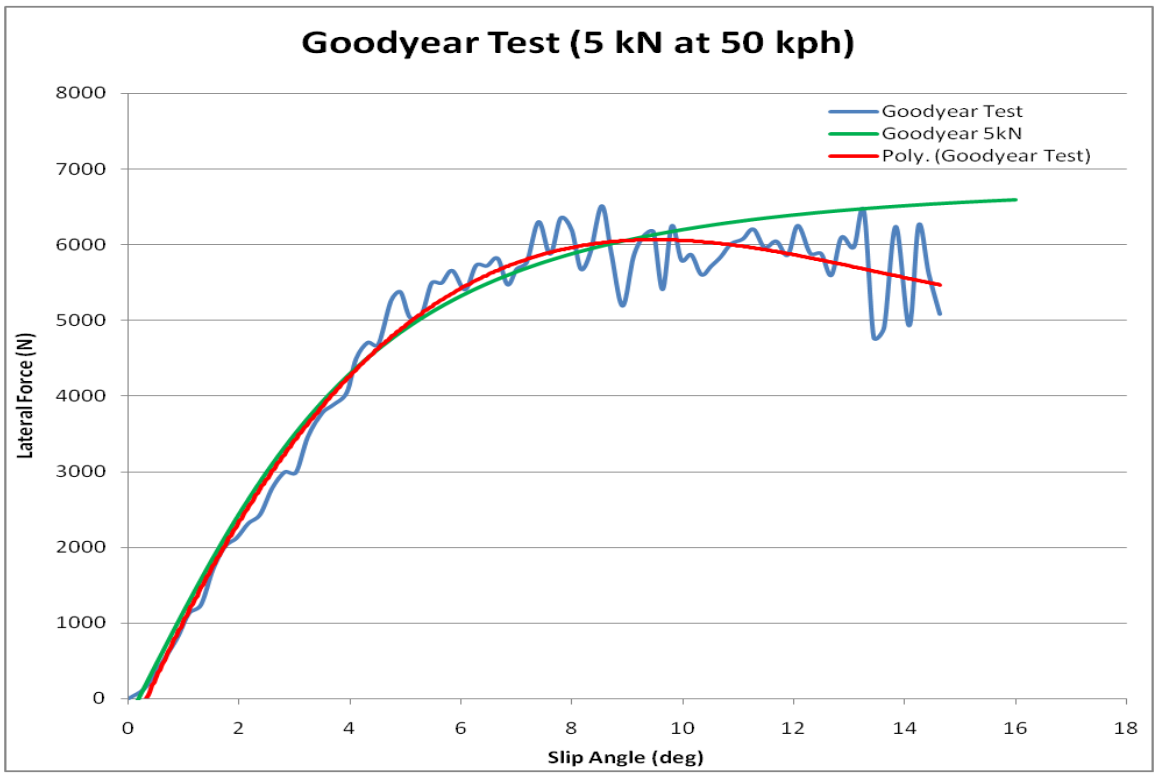

Figure 30. TTT Validation Test Run 4

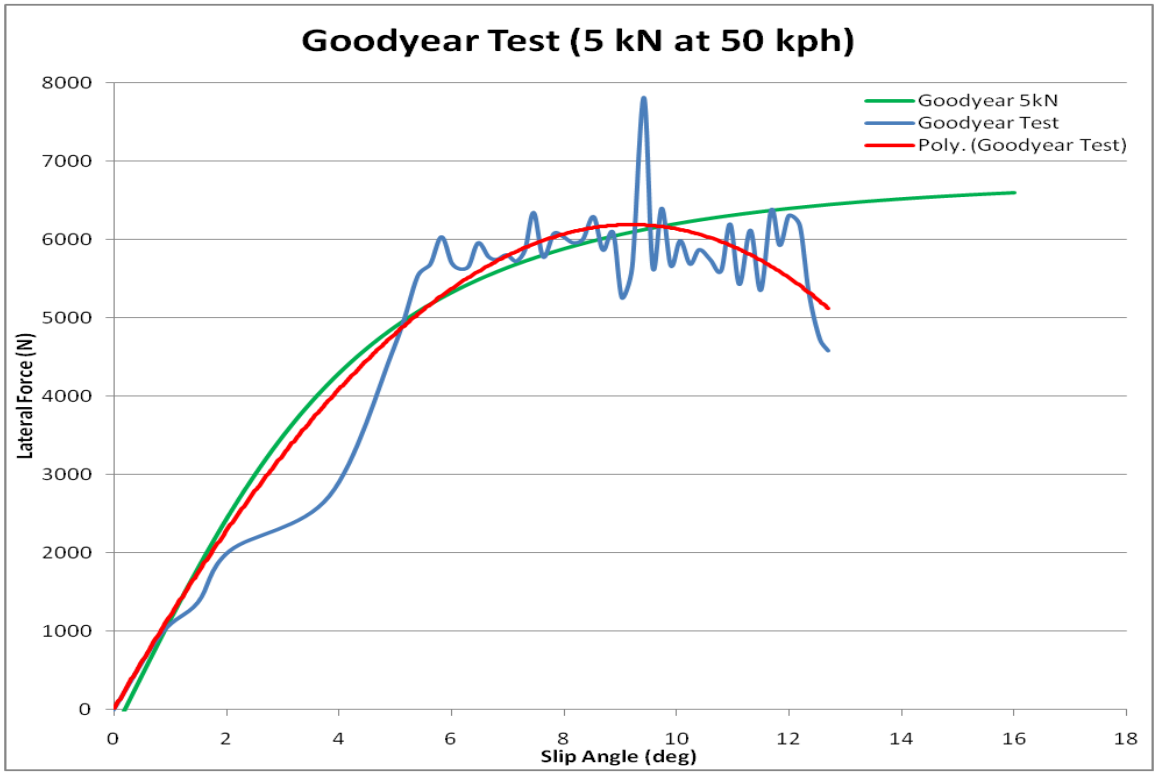

Figure 31. TTT Validation Test Run 5

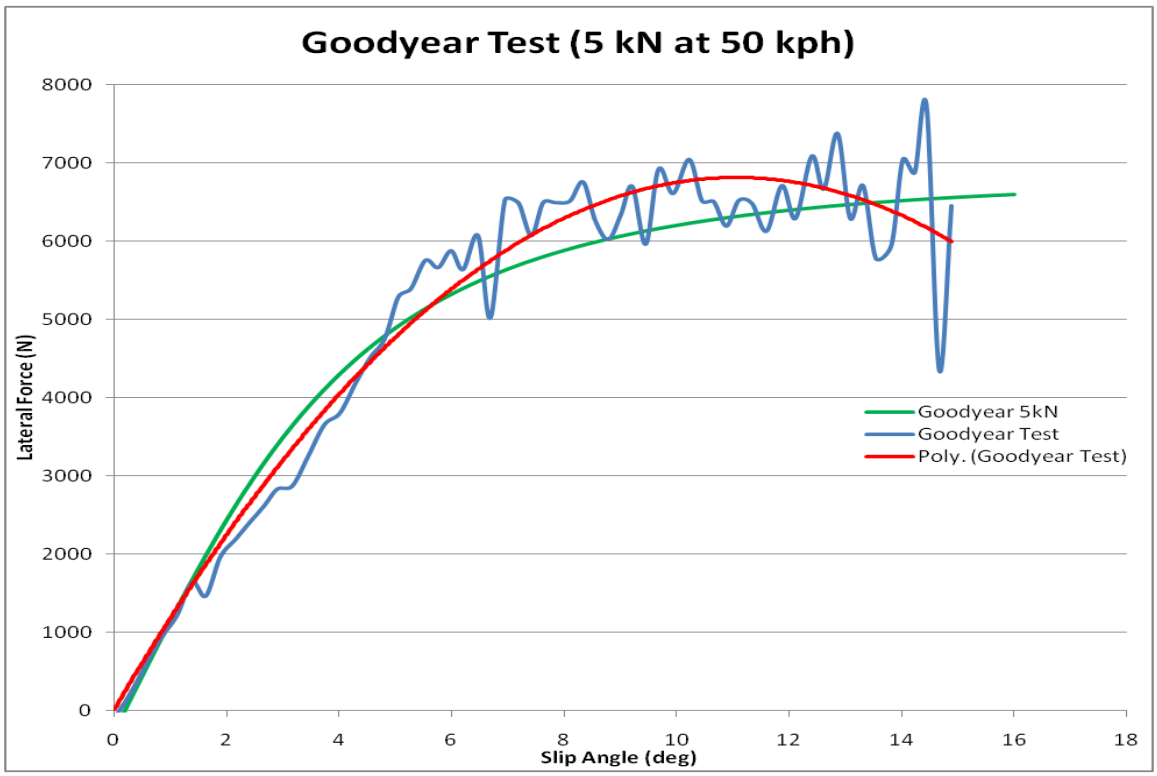

Figure 32. TTT Validation Test Run 6

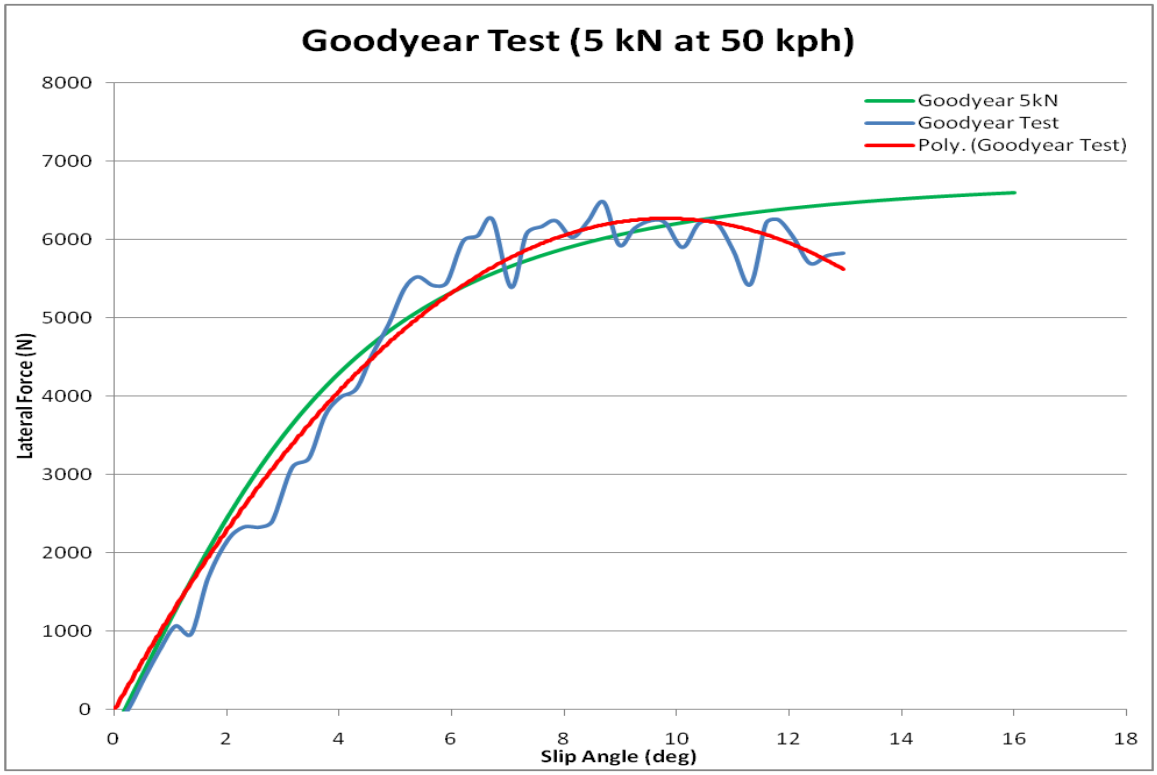

Figure 33. TTT Validation Test Run 7

3.4.2 Validation Experiment II

Validation experiment II was conducted immediately after experiment one. A second wheel with the Michelin passenger tire was mounted to the rig and testing was carried out the same as it was in the first test. The same loading cases and speeds were run in the second test so as to compare the individual tire data collected with that already known from the flat track tests. Pacejka coefficients were also given with the flat track data.

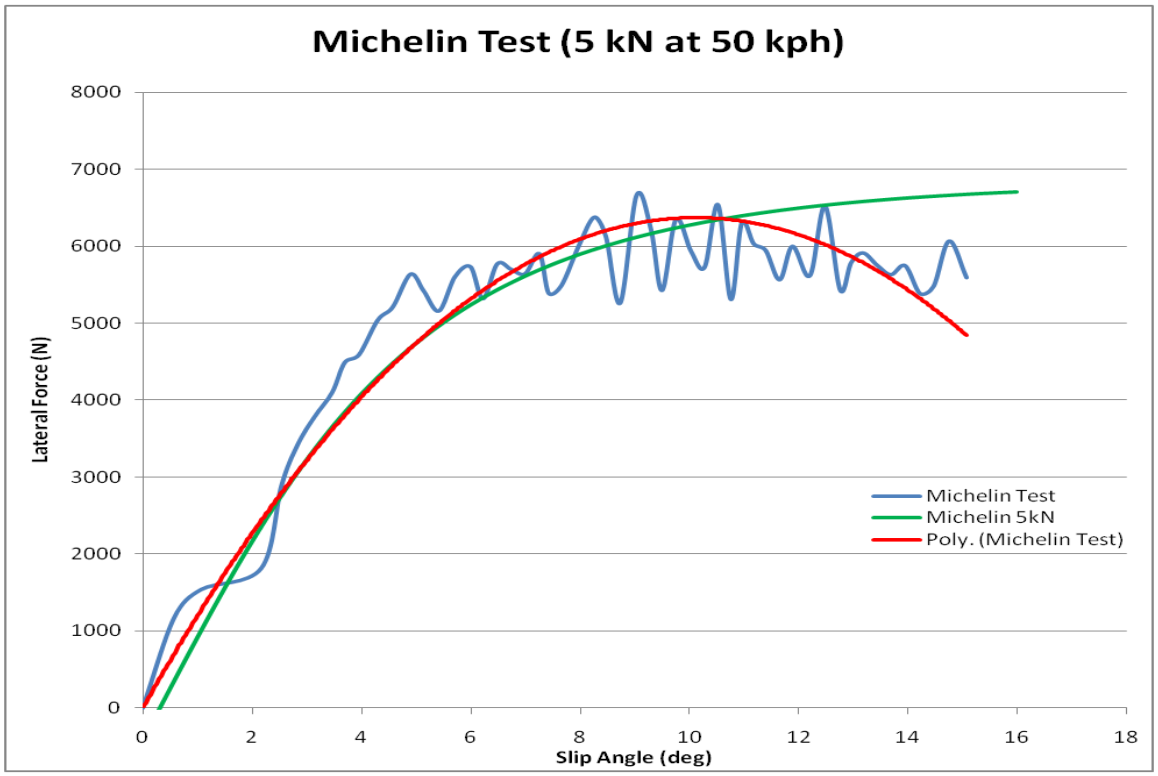

Figure 34. TTT Validation Test Run 8

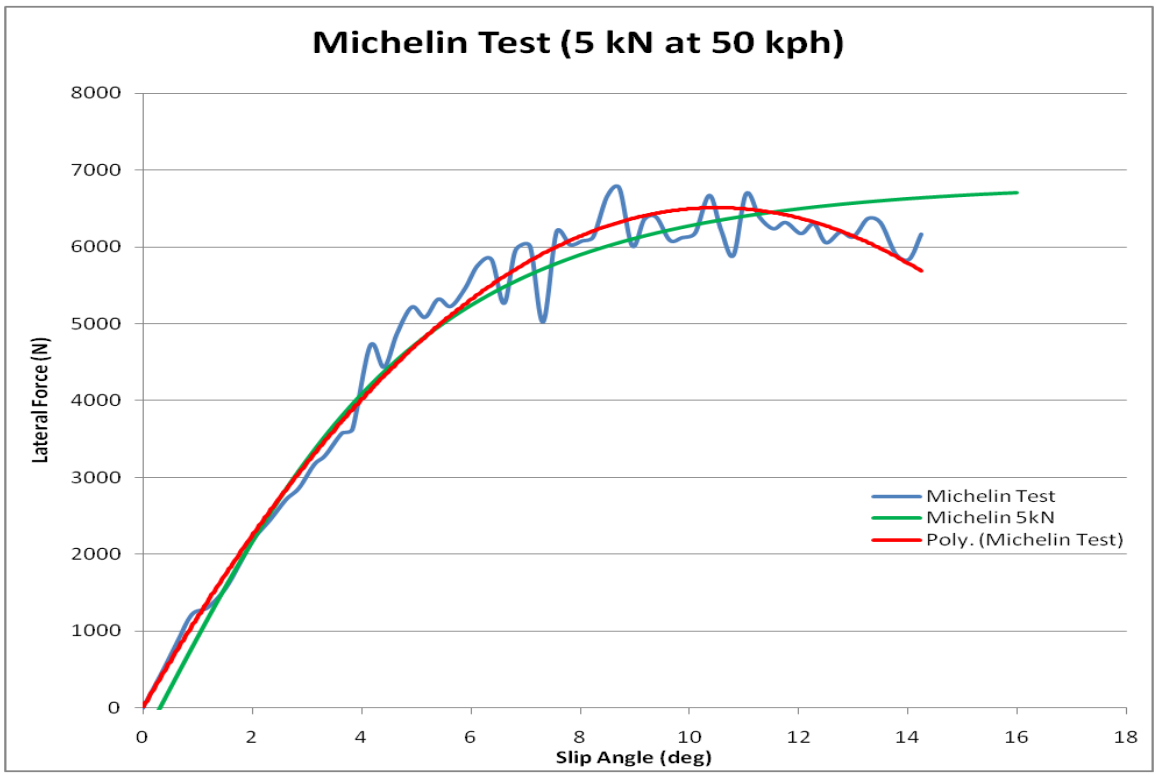

Figure 35. TTT Validation Test Run 9

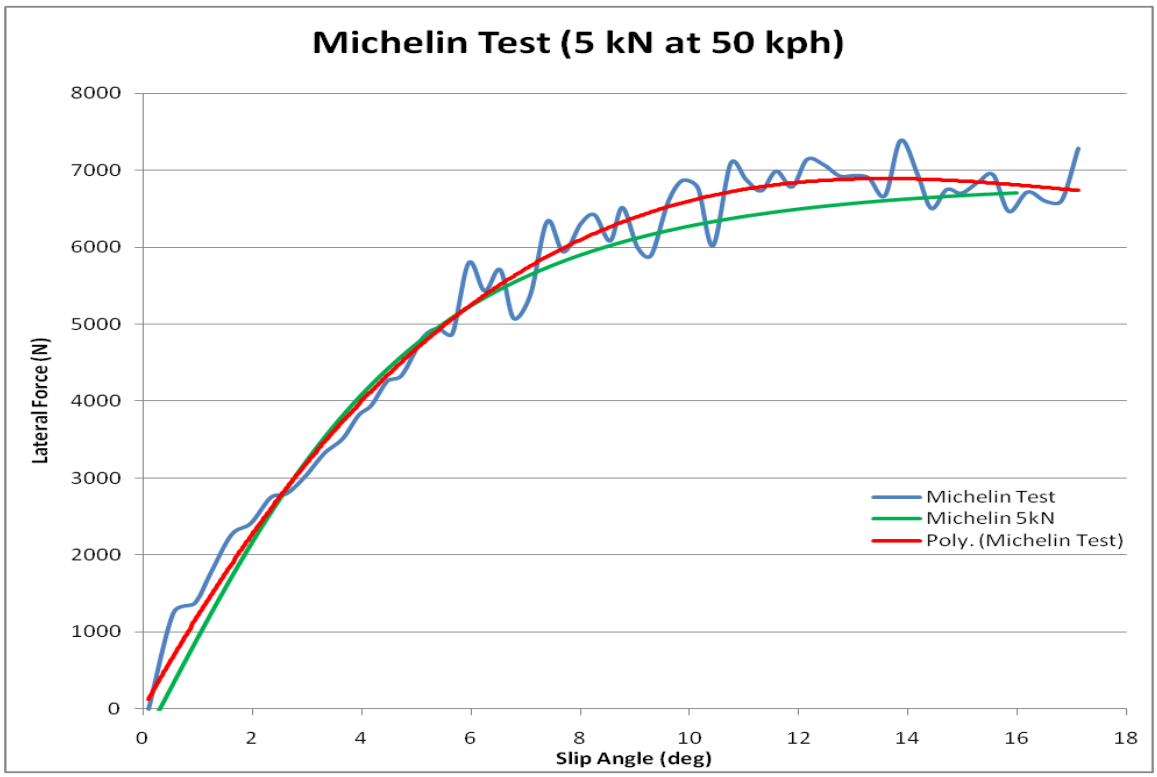

Figure 36. TTT Validation Test Run 10

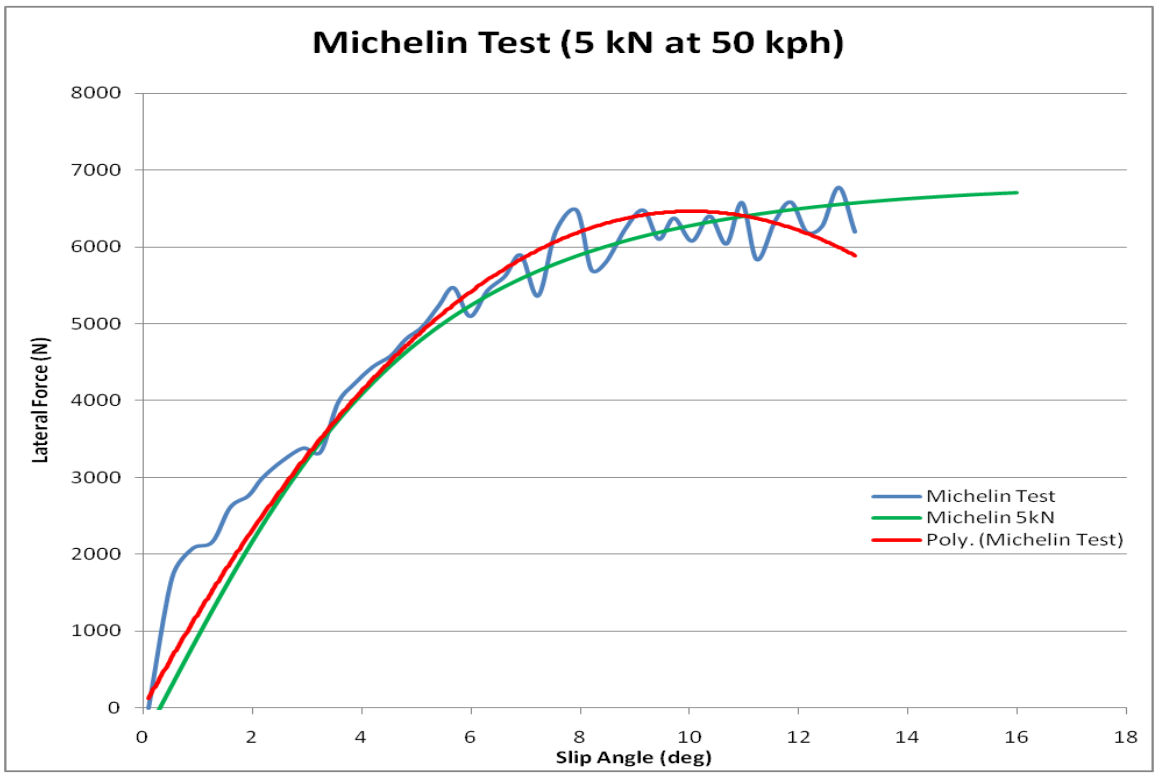

Figure 37. TTT Validation Test Run 11

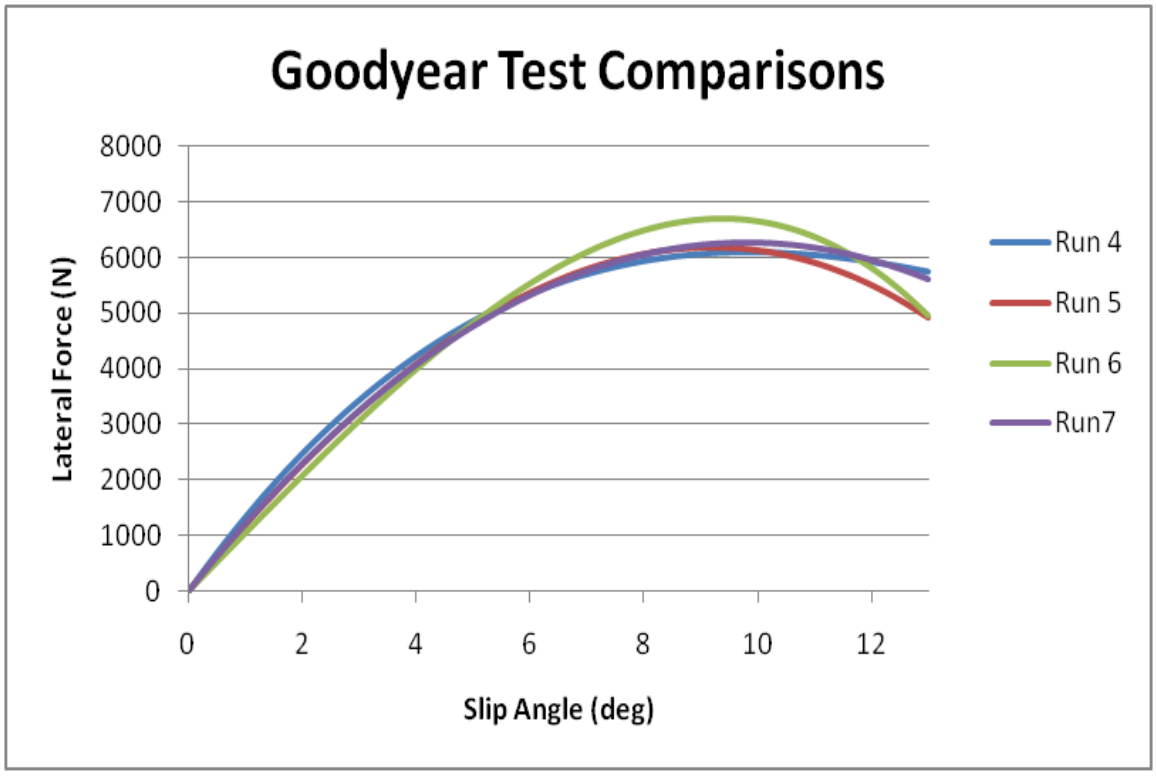

Figure 38. TTT Goodyear Tests Test Run Repeatability

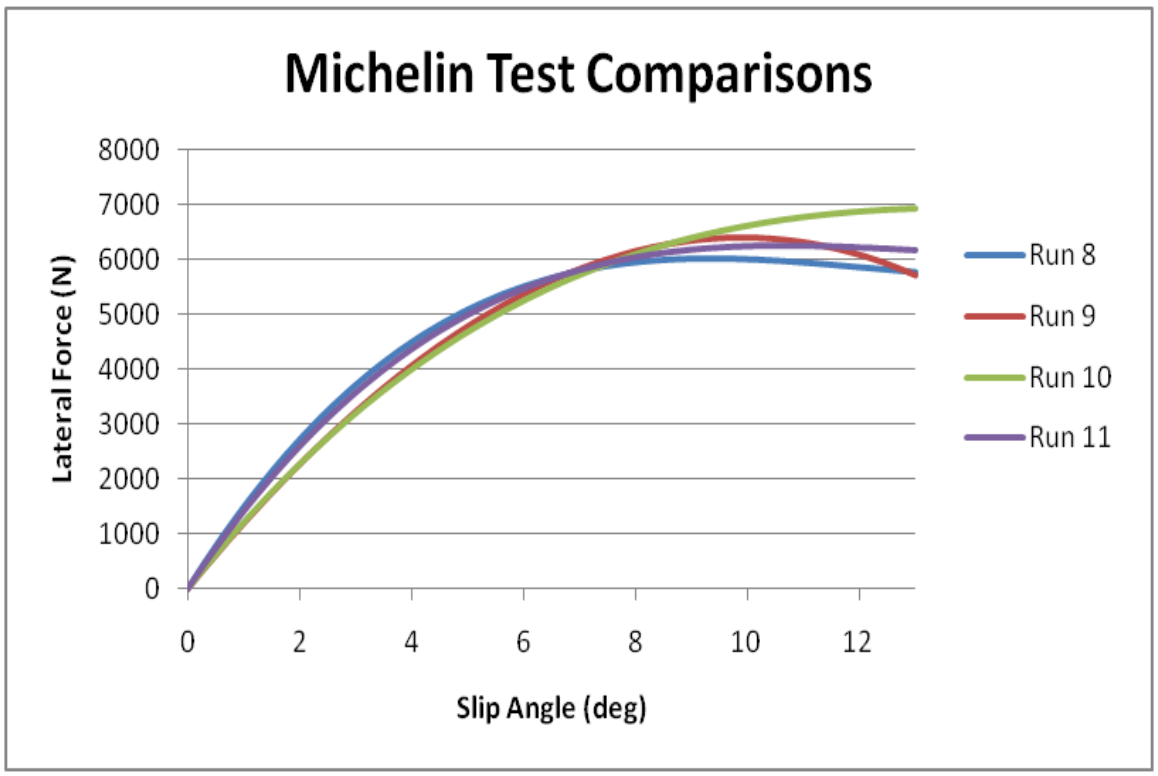

Figure 39. TTT Michelin Tests Test Run Repeatability

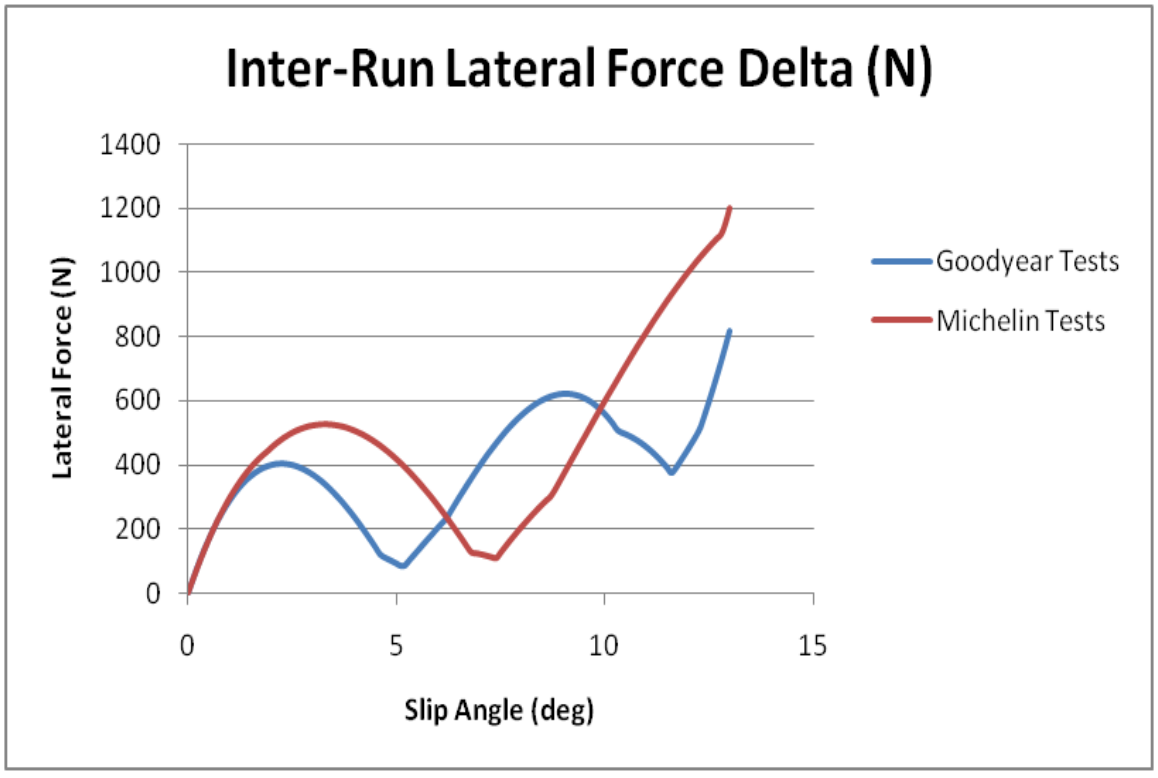

Figure 40. TTT Inter-Run Lateral Force Deltas

4. Rollover Simulation with TruckSim

4.1 Introduction

This rollover study was carried out in addition to the TTT design. It is related to the TTT design because tire data can now be more easily collected and a tire model created for use in rollover simulations. TruckSim was chosen as the simulation software for this project because of its availability. It is also a fairly simple program to operate and runs quickly, which decreases simulation time. Vehicle parameters are also easily tuned and many runs and results can be achieved with minimal time and effort.

Vehicle model setup in TruckSim is a relatively simple process. Much data is needed about the vehicle. Locations of masses, moments of inertia of the bodies, suspension geometries, kinematic suspension data, and a tire model are just some of the parameters needed to complete the vehicle model in the program. Many of these parameters, such as moments of inertia, are very difficult to come by if the modeler was not the designer, or they do not have access to much of the OEM design material. Sometimes these parameters need to be assumed or estimated. This of course is the downfall of any dynamic vehicle model; the accuracy which is required versus the completeness of the known data. TruckSim, however, does have built in starter models from which one can choose a related general model and build from. This simplifies the process but by no means is the best solution.

With a complete vehicle dynamics model, simulation work can commence. One area of increasing concern for vehicle safety is the rollover scenario. With the growing number of heavy, high CG vehicles produced for militaries and civilians, rollovers are phenomena that occur more often than they should. Ungoren, Peng, and Milot studied SUV rollover with a stability control system implemented in 2001 [26]. J-Turns and Fishhook maneuvers were used as rollover tests. These maneuvers are discussed in Chapter 4.4. Roll angle, steering angle and braking input were the studied parameters. Rajamani discusses alternative roll stability control mechanisms such as differential

braking, steer-by-wire, all wheel drive torque distribution, and active suspensions. The text provides excellent background for many different means of vehicle control [27].

4.2 Simulation and Model Setup

Accurate tire data is generally the most difficult simulation parameter to obtain. Again, this is due to the large magnitude of data and time required to gather the data. Completeness is of prime importance, and this is why extensive tire testing needs to be completed before a simulation is carried out. As previously stated, a working model can be created with some effort, or a complete model can be created with exponentially more effort. The choice is in the hands of the engineer and is based on their required level of accuracy in results. Many times simulation comparisons will suffice so a less sophisticated model is acceptable. Field testing can then be carried out after a "virtual tune" has been chosen. Other times, constraints may not allow for much physical tuning, or very accurate values may be needed directly from simulation. If this is the case, then the later tire model should be constructed with a vehicle model to match.

A stock military vehicle model was developed in accordance to specifications obtained from the project sponsor. The stock vehicle was then implemented with the active suspension model and comparisons were made between the controlled and uncontrolled vehicle on a fishhook handling maneuver. Rollover was the evaluated parameter. Vehicle rollover was studied because these vehicles are known in the field to have a relatively high amount of incidents involving a rollover situation. Vehicle stability is always an issue with high CG, heavy vehicles. But it is obviously not something the men and women driving these in a combat situation should to be concerned with. Safety is the number one goal of rollover studies as it is easy for injuries or deaths to occur. Mobility of the truck is also of high importance to the operator.

An NHTSA fishhook maneuver was chosen for these rollover simulations because it is a very common test for vehicle rollover. A fishhook maneuver consists of an initial steering wheel input to the 6.5 times the steering angle required to maintain 0.3 g on a skidpad. This steering angle is achieved at a set 720 deg/s rate. The steering wheel angle is held until a roll rate of plus or minus 1.5 deg/s is achieved. Opposite steer to the same

0.3 g steer angle is given at the same 720 deg/s. This is held for the remainder of the test [28]. Most OEMs use this maneuver to evaluate rollover since it is a standardized procedure that can be directly compared among vehicles. The simulations were performed on flat asphalt. Vehicle roll angle, tire forces, spring forces were studied. A failing run was one in which the vehicle overturned.

4.3 Control Algorithm

Simulink was used to create the control algorithm for these simulations because TruckSim has a built in interface with it. In the Simulink top level, the user connects a TruckSim block to their controller and feeds back necessary parameter values. The controller was designed and developed before simulation occurred. Tuning was done in simulation to fine tune the lookup Tables required for the controller to operate.

As seen in Figure 41 these simulations required roll angle to be fed into the controller and allowed an additional spring force to be put back into TruckSim for chassis control at the spring locations. This method only works for handling situations because there will be roll induced motion present in off-road driving or with single bump inputs. For this study however, the roll angle alone does suffice. When expanded, this signal would need to be supplemented with more signals, and implemented into a more versatile algorithm. Four spring forces were fed back into the simulation in real time to adjust the wheel forces and chassis attitude during the maneuver. Positive (upward) forces are applied to the chassis side furthest from the turn center, and negative chassis forces are applied to the opposite spring locations. These negative forces are not possible with a semi-active damper system or a passive damper system.

The idea of this control is to stop, and reverse, the outward migration of the CG thus decreasing the overturning moment on the chassis based on CG location and inertia. It is easiest to model this additional force as a spring force due to the design of TruckSim. This hypothetical spring force could realistically take the shape of a fully active suspension system, a controllable anti-roll bar, or any other means of inducing positive and negative forces onto the chassis in real time. Additional variables were sent to the workspace for Matlab calculations and checks. The simulation was run at 50 kph because

that is the speed at which the stock passive system fails. This speed was found experimentally in simulation. The purpose of these simulations was to theoretically demonstrate that large vehicle rollover can be controlled with the use of an active suspension system and not to provide a hardware solution to the problem.

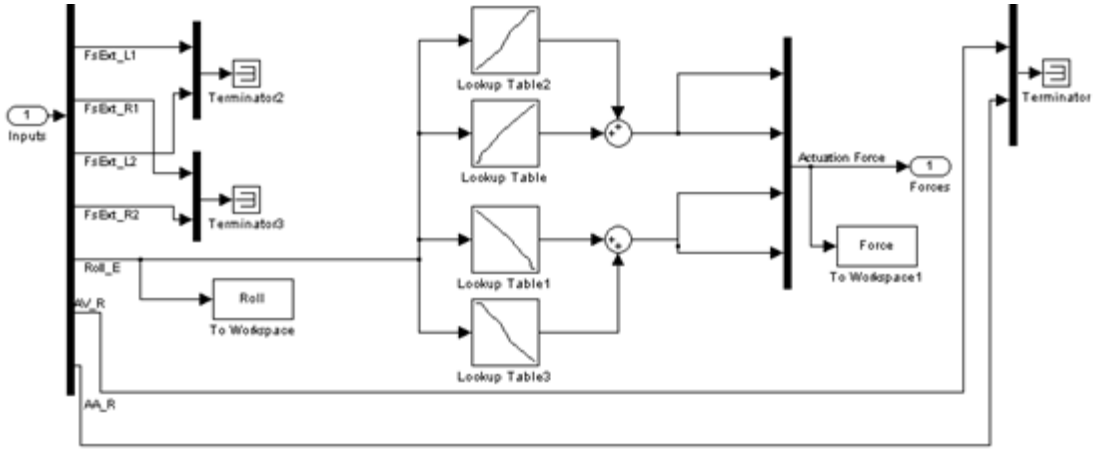

Figure 41. Simulink Controller.

This thesis' solution to vehicle rollover was to use a feedback active suspension controller because I believe that safety issues can arise any time braking or steering control is removed from the driver. Non-linear feedback control was chosen with lookup Tables for these simulations due to its simplicity and ease of integration. Linear control would simply mimic a standard anti-roll bar. Tuning is limited with this method based on the number of rows that the user inputs into the lookup Tables. Lookup Tables were developed by multiple "trial and error" tuning sessions and are shown in Table 2 below. They are easier to implement than an equation because of the non-linear model. The lookup Tables linearly interpolate between points to create other values. The controller does not currently adapt to special case scenarios, so it is also limited in this sense.

Table 2. Chassis Controller Force Value Lookup Table.

	Lookup Table Values	
Chassis Roll Angle	Positive Force (N)	Negative Force (N)
0	0	0
0.25	5000	
0.5	7500	0
1	10000	-5000
2	15000	-10000
3	20000	-20000
5	30000	-30000

4.4 Simulation Case Studies

The data plots presented below were pulled from the simulation software directly. There is no post-processing involved since TruckSim has its own internal plotting program.

The fishhook maneuver used was created as an event in TruckSim which commands the steering wheel angle, and a "perfect" driver is assumed. This eliminates the variance between runs. Legend entries labeled as "Non-Active Spring Sim" represent the stock vehicle without the control algorithm implemented and "Active Spring Sim" legend entries represent the vehicle with the control implementation. Figure 42 is the steering wheel angle command and is the same for both cases to keep consistency and comparability.

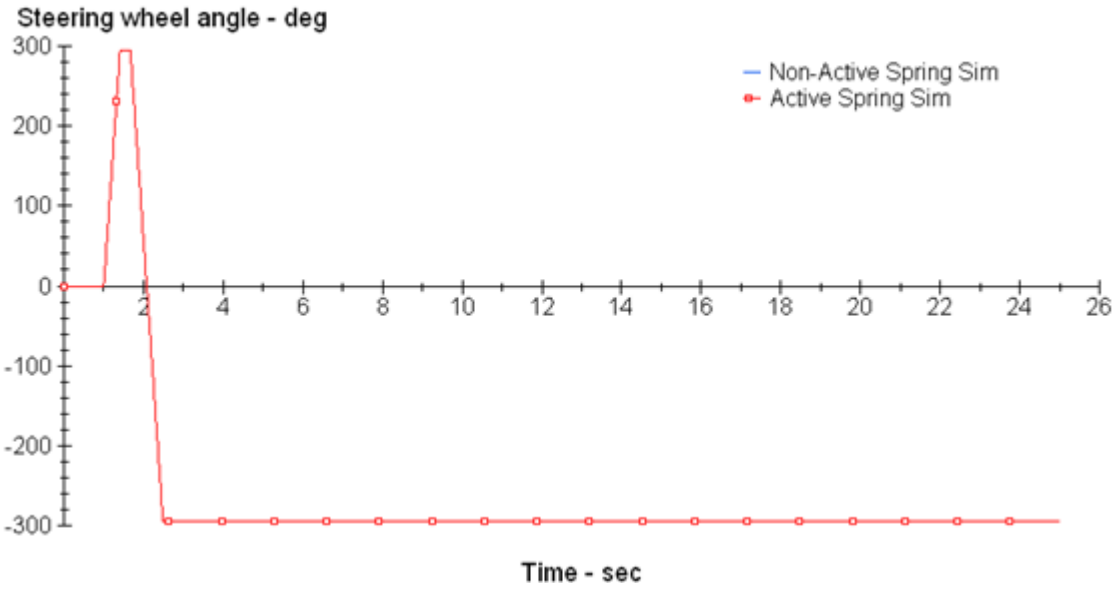

Figure 42. Vehicle Steering Wheel Angle from TruckSim.

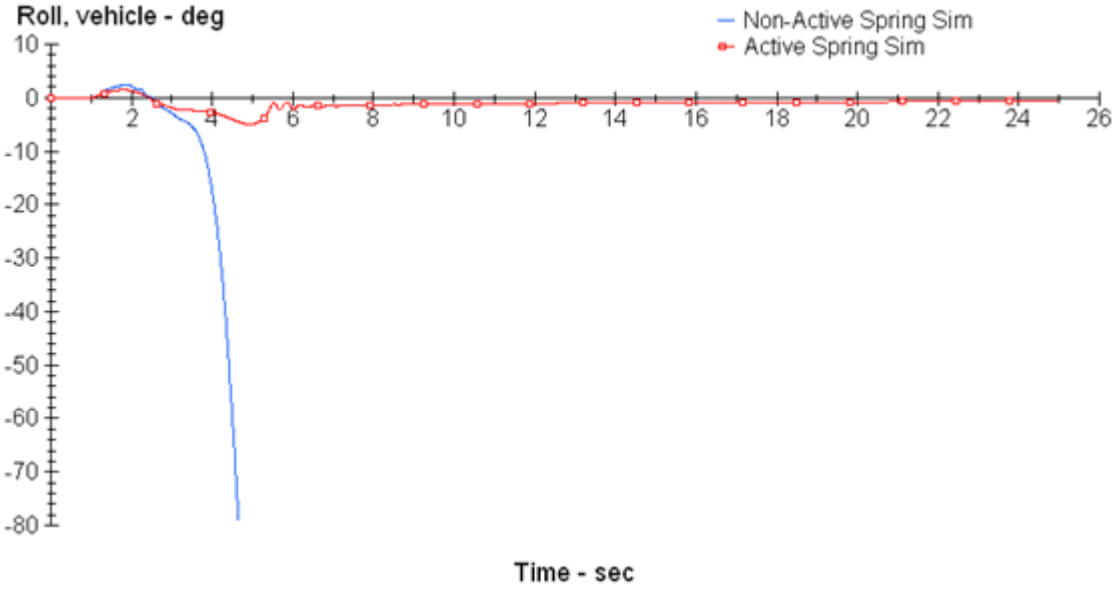

Figure 43. Vehicle Roll Angle from TruckSim.

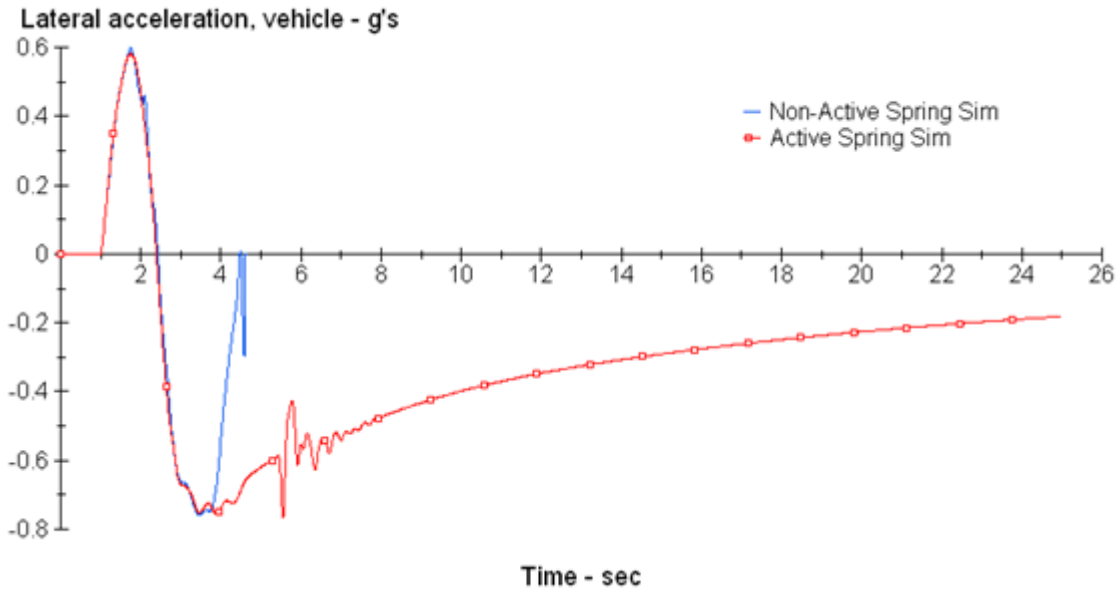

Figure 44. Lateral Acceleration from TruckSim.

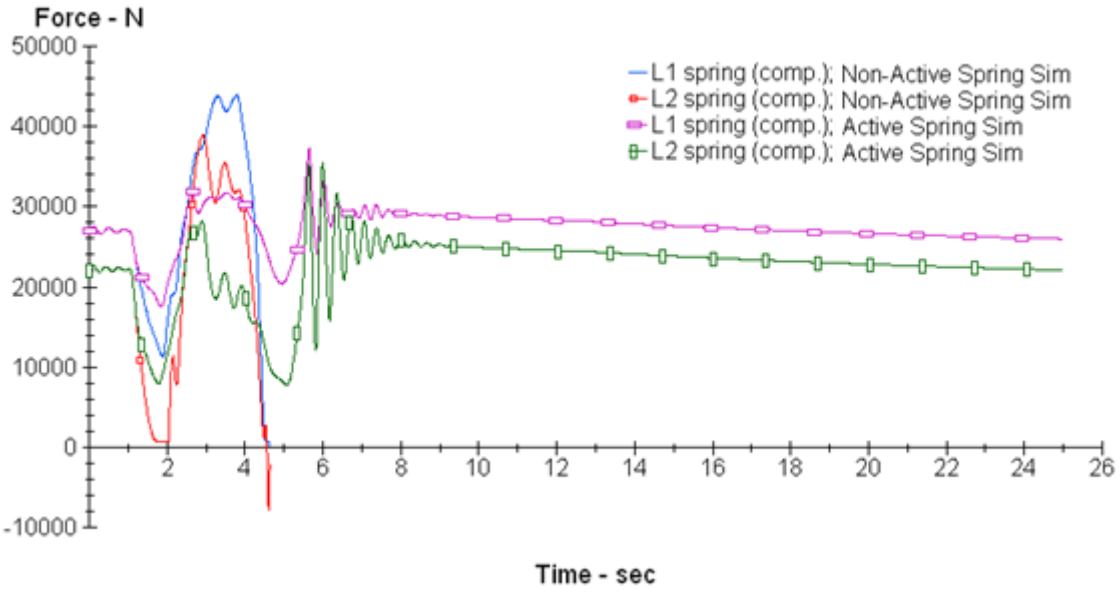

Figure 45. Left Side Spring Forces from TruckSim.

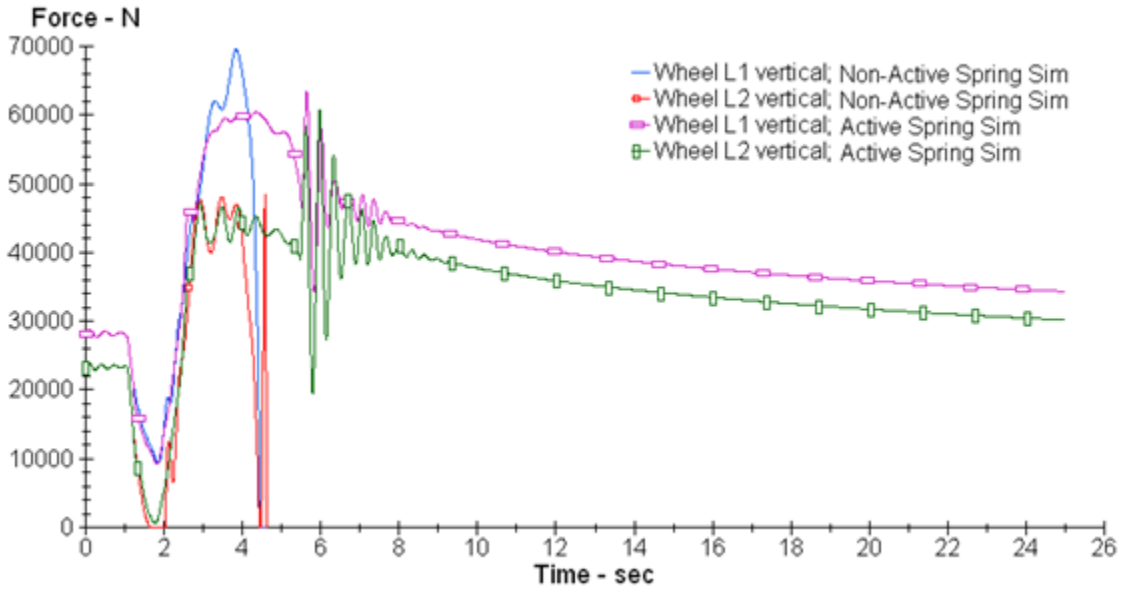

Figure 46. Left Side Tire Vertical Forces from TruckSim.

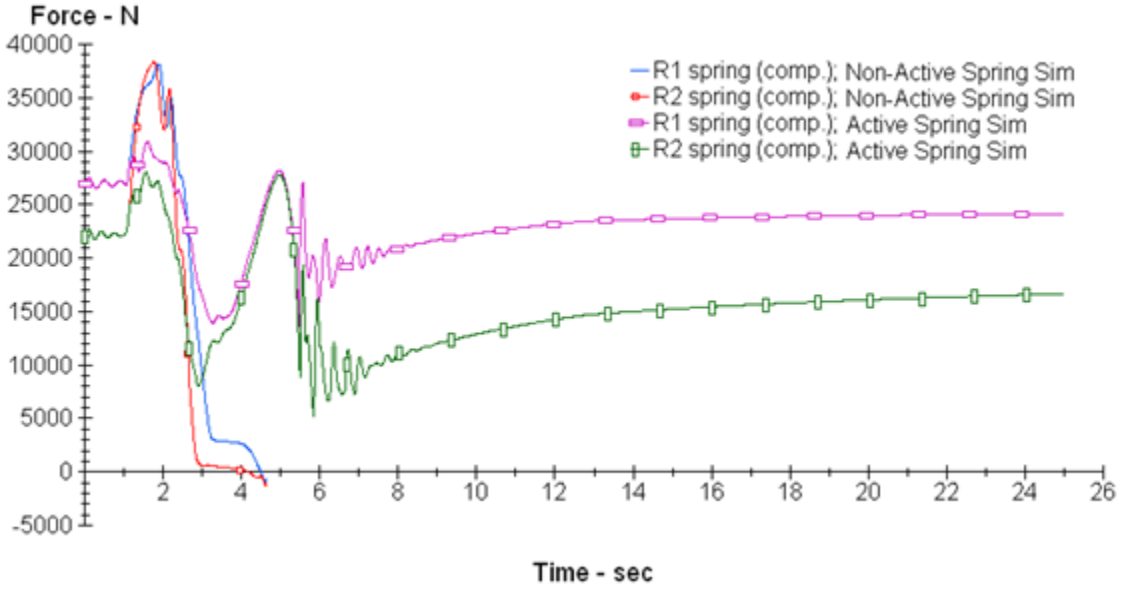

Figure 47. Right Side Spring Forces from TruckSim.

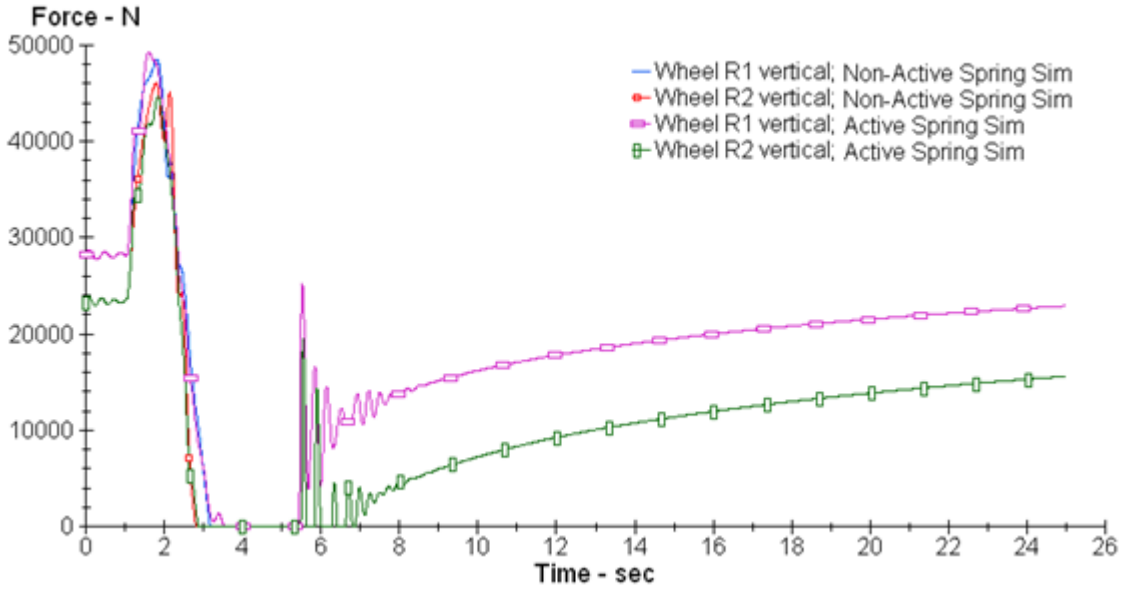

Figure 48. Right Side Tire Vertical Forces from TruckSim.

4.5 Simulation Conclusions

Vehicle rollover is shown in the stock passive system by the vehicle roll angle drop-off around 4 seconds in Figure 43. Wheel vertical forces are also shown and can be seen to go to zero at this point. The objective of this simulation was to stop rollover at any cost of vehicle or passenger discomfort, meaning that this control method will likely provide a harsh ride when activated.

Based on the criteria for rollover being that the vehicle does in fact overturn, it can easily be seen that the control method does work. It effectively prevents the vehicle from rolling by changing the forces acting on the chassis. This is accomplished by applying a negative force to suspension closer to the inside of the turn, and applying a positive force to the suspension closer to the outside of the turn. This effectively rolls the vehicle into the turn instead of the natural opposite. Shown in Figure 47, spring force in the inside suspension begin to drastically drop off, indicating the beginning of rollover. The controller sees the changing roll angle and begins reversing this roll by pushing up on the outside of the chassis, and pulling down on the inside. Spring force then begins to build back up on the inside suspension. The right side tire vertical forces shown in Figure 48 insist that inside tires do still lift off the ground, if only by a couple of inches. This

could cause the vehicle to fail the fishhook maneuver criteria, so more tuning should be completed.

As expected by this control method, the linear interpolation between points and the magnitude of forces involved does upset the chassis and oscillation of the suspension force occurs until a stable roll angle is obtained. The passengers of the truck would not be comfortable during the system's activation but that could be reduced by a different type of control and much more tuning time with focus on ride quality. Other scenarios, such as a tripped rollover, were not studied and are outside the scope of this thesis.

5. Conclusions and Future Work

In conclusion, the TTT design project was successful in that it met its design goals and provided a means of providing a simple means of obtaining tire data. The results as shown were repeatable and very similar to flat track testing results. This proves that the TTT is a valid piece of testing equipment.

This project was completed over the span of one year. More time could provide a broader testing and results base. The first recommendations for future work would be to Study TTT data to see if the force variations can be minimized. Then the load frame should be outfit with multiple accelerometers and PSDs could be made to study vibration modes. A more controlled launching strategy for the tow vehicle should also be created. The water tank should be filled and thoroughly tested full and while wet testing to study the effects of tongue load and tow truck stability. A braking system should be added to give the TTT a means of providing for slip ratio. The generator should be mounted inside of the trailer with a means for exhausting the engine fumes since loading it into the bed increases start-up time due to not being able to store the generator in the truck. It must currently be loaded in the truck each time the rig is used. The generator would also then provide some additional ballast. The water tank should also be baffled in order to decrease water sloshing effects when not completely full. Other useful sensors to add to the TTT would be a multipoint infrared temperature sensor aimed at the tire and the ground. These temperatures would be recorded with the force and moment data. A database of tire test runs could then be completed with the current tires on alternative road surfaces such as sand, grass, snow, and gravel in order to develop Pacejka models for use with off-road simulations.

The rollover study control algorithm was ultimately a successful venture. The speed at which the studied vehicle rolled over was increased at the cost of passenger ride comfort. The cost of such a system's implementation should be considered as the design and integration of any active suspension system is much more costly than a passive system.

For future work on the rollover simulation study it is recommended that a more robust and expandable controller be implemented that can accommodate certain special

cases such as off-road maneuvers, off-road terrains, other handling maneuvers, and possibly speed sensitive situations. Many more signals could be fed back in order to increase the tune-ability of the system such as steering wheel angle, suspension position sensors, speeds, accelerations, and angular rates. These would be included in similar fashion to the roll angle sensor but would require further development of the algorithm and tuning to determine the optimal setup.

References

1. “Vehicle Dynamics Terminology” SAE J670e, Society of Automotive Engineers, Inc., Warrendale, PA, July 1976.
2. Pacejka, H.B., “Tyre and Vehicle Dynamics”, SAE International, ISBN 0768017025, 2005.
3. J.A. Cabrera, A. Ortiz, A. Simon, F. Garcia and A. Perez De La Blanca: A Versatile Flat Track Tire Testing Machine. *Vehicle System Dynamics.* 40, No. 4 (2003), pp. 271–284.
4. Stocker, M.: A Giant Stride in Tire Testing. *Automotive Engineering*, 99 (1991), pp. 29–31.
5. Haney, Paul, “The Racing and High Performance Tire”, SAE International, ISBN 0768012414, 2003.
6. Helsinki University of Technology, Laboratory of Automotive Engineering; Longitudinal Friction Measurement Trailer. (2002), pp 1-5.
7. Wennstrom, Joakim. (2007), “Tire Friction on Ice; Development of testrig and roughness measurement method”. Lulea University of Technology Master’s Thesis.
8. K.P. Self, J.D.Summers, J.G.Greenlee, G.L.McLaughlin; A Mobile Off-Road Tire Test Apparatus. *Applied Engineering in Agriculture*, Vol. 4. (1988), pp. 2-4.
9. G Phetteplace, S. Shoop, T. Slagle: Measuring Lateral Tire Performance on Winter Surfaces. *Tire Science and Technology*, TSTCA, Vol. 35, No. 1, January-March 2007, pp. 56-68.
10. Hydraulic Loading System for Aircraft Wheel Test Rig. *Fluid Power International*, 38(1973), pp.17-19.
11. Peter Lugner, Hans Pacejka, and Manfred Plochl: Recent advances in tyre models and testing procedures. *Vehicle System Dynamics.* 43, No. 6-7(2005), pp. 413-436.
12. Salaani, Mohamed Kamel, “Analytical Tire Forces and Moments with Physical Parameters,” *Tire Society and Technology*, TSTCA, Vol. 36, No. 1, January-March 2008, pp. 3-42.
13. E.R Gardner, “Tyres;general developments, materials, manufacture” *Progress of Rubber Technology*, 38, 1975, pp. 35-37.
14. Shigley, Mischke, Budynas, “Mechanical Engineering Design”, McGraw-Hill, ISBN 0072520361, 2004.
15. Kistler Instrumente AG: RoaDyn® P530 Measuring Hub for Tire- and Wheel Test Benches. pp. 1-5. 2008
16. *www.kistler.com*. Kistler. 24 November, 2009.
17. *www.parkermotion.com*. Parker Hannifin. 24 November, 2009.
18. Milliken, Milliken, “Race Car Vehicle Dynamics”, SAE International, ISBN 1560915269, 1995.
19. Wong, J.Y., “Theory of Ground Vehicles”, Wiley, ISBN 0471354619, 2001.
20. *www.motioncontrol.com*. Nabtesco Motion Control. 24 November, 2009.
21. Winkler, Chris. (personal communication. February, 2009).
22. *www.firestoneindustrial.com*. Firestone Industrial. 24 November, 2009.
23. *www.tank-depot.com*. Tank Depot. 24 November, 2009.
24. *www.mcmaster.com*. McMaster-Carr. 24 November, 2009.
25. *www.millerwelds.com*. Miller Electric. 24 November, 2009.

26. Ali Y. Ungoren, Huei Peng, and Danny R. Milot: Rollover Propensity Evaluation of an SUV Equipped with a TRW VSC System. Society of Automotive Engineers. 2001-01-0128. pp. 1-9.
27. Rajamani, Rajesh, "Vehicle Dynamics and Control", Springer, ISBN 0387263969, 2006.
28. Department of Transportation, National Highway Traffic Safety Administration: Consumer Information; New Car Assessment Program; Rollover Resistance. NHTSA-2001-9663, (2001)

Appendix A - Component Specifications

Table 3. Kistler Hub Specification Table.

Technical Data

Measuring range	F_x, F_y	kN	–20 ... 20[1]
	F_z	kN	0 ... 30[1]
	M_x	kN·m	–7,5 ... 7,5
	M_y	kN·m	–3 ... 3
	M_z	kN·m	–1,3 ... 1,3
Calibrated partial range	F_x, F_y	kN	0 ... 2
	F_z	kN	0 ... 3
Overload	F_x, F_y	kN	–30/30
	F_z	kN	–42/42
Sensitivity	F_x	pC/N	≈–8
	F_y	pC/N	≈–3,7
	F_z	pC/N	≈–8
Linearity	F_x, F_z, F_y	% FSO	≤±0,5
Hysteresis	F_x, F_z, F_y	% FSO	≤0,5
Crosstalk	F_y –> F_x, F_z	%	≤±1,5
	F_x <–> F_z	%	≤±1,5
	F_x, F_z –> F_y	%	≤±2
Natural frequency	f_n (x,z)	Hz	≈2 400
	f_n (y)	Hz	≈2 100
Maximum speed		min^{-1}	≤2 000
Operating temperature range		°C	–20 ... 70

Insulation resistance		Ω	$>10^{13}$
Ground insulation		Ω	$>10^{8}$
Degree of protection according to DIN40050			IP65
Dimension			
diameter		mm	298
length		mm	337
Weight		kg	72

Requirements for Oil Lubrication

Inlet pipe		number	2
	di/da	mm	6/8
Oil pressure[2]	p	bar	≤0,5
Flow rate/per inlet pipe	$\hat{V}$	l/min	1
Flow rate/total	$\hat{V}$	l/min	2
Kinematical viscosity (@40°)	ν	mm^2/s	20 ... 25
Outlet pipe		number	2
	di/da	mm	8/12
Oil pressure	p	bar	pressureless

[1] with standard force application point at tire radius R = 300 mm and press-in depth e = 38 mm.

[2] Pressure-control valve is recommended.

Table 4. Servo Motor Specification Table.

Size 34, Encoder Feedback, Specifications

Parameter	Symbol	Units	BE341F	BE341J	BE342H	BE342K	BE343J	BE343L	BE344J	BE344L
Stall Torque Continous[1]	T_{cs}	lb-in	15.0	14.9	25.3	25.7	35.6	35.4	43.3	42.9
		oz-in	241	239	406	411	570	566	693	686
		Nm	1.68	1.67	2.84	2.88	3.99	3.96	4.85	4.80
Stall Current Continuous[1,4,8]	I_{cs}(sine)	Amps Peak	5.1	10.4	6.9	13.5	9.9	15.8	9.1	14.3
Stall Current Continuous[1,7]	I_{cs}(trap)	Amps DC	4.5	9.0	5.9	11.7	8.6	13.7	7.8	12.4
Peak Torque[6]	T_{pk}	lb-in	45.1	44.8	76.0	77.1	106.9	106.1	129.9	128.6
		oz-in	722	717	1217	1233	1710	1697	2078	2058
		Nm	5.05	5.02	8.52	8.63	11.97	11.88	14.55	14.40
Peak Current[4,6,8]	I_{pk}(sine)	Amps Peak	15.4	31.3	20.6	40.4	29.8	47.4	27.2	43.0
Peak Current[6,7]	I_{pk}(trap)	Amps DC	13.4	27.1	17.8	35.0	25.8	41.0	23.5	37.3
Rated Speed[2]	ω_r	rpm	4625	5000	4500	5000	4375	5000	3500	5000
Current @ Rated Speed	I_r(sine)	Amps Peak	4.2	8.3	5.5	10.3	7.8	11.5	7.6	9.9
Current @ Rated Speed	I_r(trap)	Amps	3.7	7.2	4.8	8.9	6.8	9.9	6.6	8.5
Torque @ Rated Speed	T_r	lb-in	11.9	11.4	20.3	19.1	27.7	24.8	35.6	28.5
		oz-in	191	182	325	305	443	397	569	456
		Nm	1.34	1.27	2.28	2.14	3.10	2.78	3.98	3.19
Shaft Power @ Rated Speed	P_o	watts	653	673	1082	1128	1434	1468	1473	1686
Voltage Constant[3,4]	K_b	Volts/rad/s	0.382	0.187	0.483	0.249	0.468	0.292	0.624	0.390
Voltage Constant[3,4]	K_e	Volts/Krpm	40.00	19.58	50.58	26.08	49.01	30.58	65.35	40.84
Torque Constant[9]	K_t(sine)	oz-in/Amp Peak	46.84	22.93	59.23	30.53	57.39	35.81	76.52	47.83
		Nm/Amp Peak	0.328	0.161	0.415	0.214	0.402	0.251	0.536	0.335
Torque Constant[3,4]	K_t(trap)	oz-in/Amp DC	54.09	26.48	68.39	35.26	66.27	41.35	88.36	55.22
		Nm/Amp DC	0.379	0.185	0.479	0.247	0.464	0.289	0.619	0.387
Resistance[3]	R	Ohms	2.59	0.63	1.70	0.44	0.96	0.38	1.23	0.49
Inductance[5]	L	mH	35.40	7.07	21.50	5.84	15.09	6.86	20.17	7.32
Maximum Bus Voltage	V_m	Volts DC	340	340	340	340	340	340	340	340
Thermal Res Wind-Amb	R_{th} w-a	°C/watt	1.40	1.40	1.20	1.20	1.01	1.01	0.95	0.95
Motor Constant	K_m	oz-in/√watt	33.61	33.36	52.45	53.15	67.64	67.07	79.67	78.89
		Nm/√watt	0.235	0.234	0.367	0.372	0.473	0.470	0.558	0.552
Viscous Damping	B	oz-in/Krpm	1.1	1.1	1.3	1.3	1.7	1.7	2.0	2.0
		Nm/Krpm	7.6E-03	7.6E-03	9.3E-03	9.3E-03	1.2E-02	1.2E-02	1.4E-02	1.4E-02
Static Friction	T_f	oz-in	1.7	1.7	2.7	2.7	4.2	4.2	5.0	5.0
		Nm	1.2E-02	1.2E-02	1.9E-02	1.9E-02	2.9E-02	2.9E-02	3.5E-02	3.5E-02
Motor Thermal Time Constant	τ_{th}	minutes	21.6	21.6	25.0	25.0	28.3	28.3	33.3	33.3
Electrical Time Constant	τ_{elec}	millisecs	13.67	11.22	12.65	13.27	15.72	18.05	16.40	14.94
Mechanical Time Constant	τ_{mch}	millisecs	0.5	0.5	0.4	0.4	0.3	0.3	0.3	0.3
Intermittent Torque Duration[10]	T_{2x}	seconds	65	65	78	78	116	116	127	127
Peak Torque Duration[11]	T_{3x}	seconds	24	24	27	27	37	37	38	38
Rotor Inertia	J	lb-in-sec²	2.7E-04	2.7E-04	4.4E-04	4.4E-04	6.1E-04	6.1E-04	7.2E-04	7.2E-04
		kg-m²	3.1E-05	3.1E-05	5.0E-05	5.0E-05	6.9E-05	6.9E-05	8.1E-05	8.1E-05
Number of Poles	Np		8	8	8	8	8	8	8	8
Motor Weight	#	lbs	4.8	4.8	7.1	7.1	9.4	9.4	11.7	11.7
		kg	2.2	2.2	3.2	3.2	4.3	4.3	5.3	5.3
Winding Class			H	H	H	H	H	H	H	H

1 *@ 25°C ambient, 125°C winding temperature, motor connected to a 10"x10"x1/4" aluminum mounting plate. @40°C ambient derate phase currents and torques by 12%.*
2 *Operation with 340 VDC bus. Maximum speed is 5000 RPM. For higher speed operation please call the factory.*
3 *Measured Line to Line, +/- 10%.*
4 *Value is measured peak of sine wave.*
5 *+/-30%, Line-to-Line, inductance bridge measurement @1Khz.*
6 *Initial winding temperature must be 60°C or less before peak current is applied.*
7 *DC current through a pair of motor phases of a trapazoidally (six state) commutated motor.*
8 *Peak of the sinusoidal current in any phase for a sinusoidally commutated motor.*
9 *Total motor torque per peak of the sinusoidal amps measured in any phase, +/-10%.*
10 *Maximum time duration with 2 times rated current applied with initial winding temp at 60°C.*
11 *Maximum time duration with 3 times rated current applied with initial winding temp at 60°C.*

Table 5. Air Spring Force Table.

Force Table (Use for Airstroke® actuator design)						
Assembly Height (in.)	Volume @ 100 PSIG (in^3)	Pounds Force				
		@20 PSIG	@40 PSIG	@60 PSIG	@80 PSIG	@100 PSIG
10.0	809	950	1,810	2,830	3,810	4,840
9.0	752	1,170	2,260	3,460	4,670	5,880
8.0	685	1,310	2,590	3,940	5,350	6,700
7.0	610	1,430	2,900	4,390	5,950	7,450
6.0	529	1,540	3,170	4,780	6,470	8,110
5.0	442	1,640	3,380	5,100	6,880	8,630
4.0	349	1,730	3,520	5,340	7,180	9,020

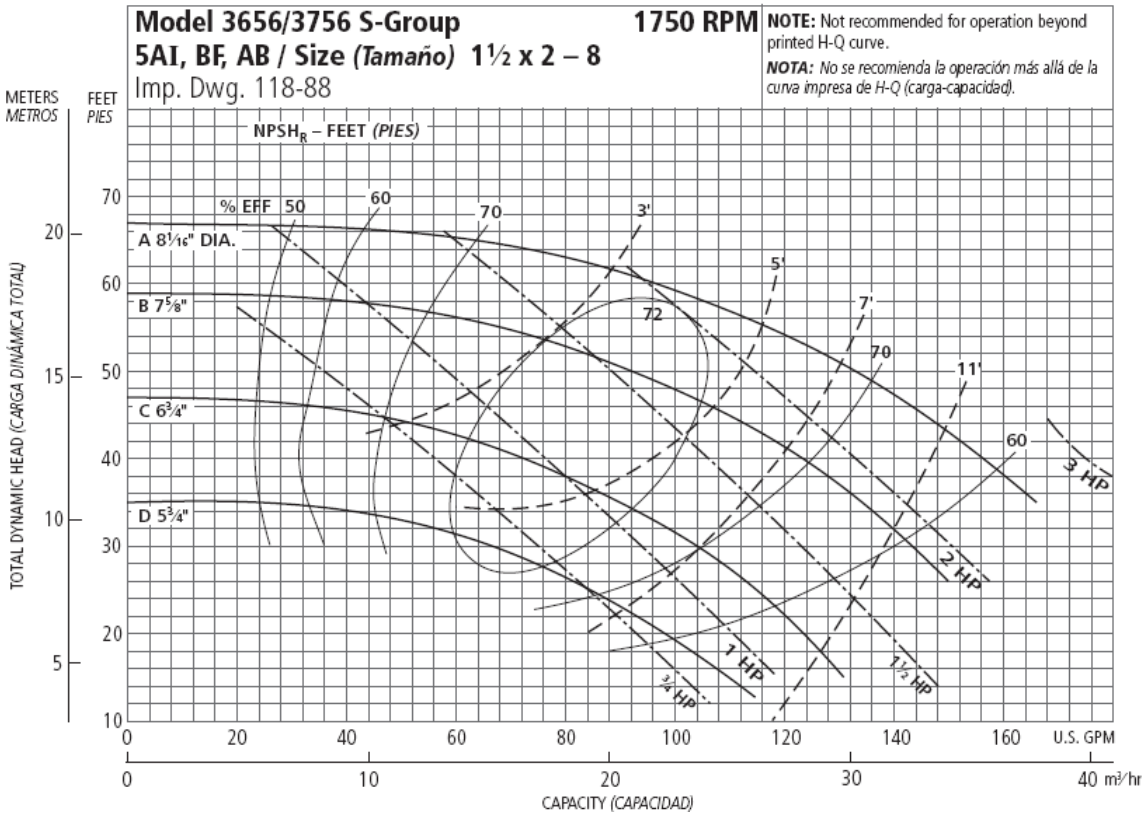

Figure 49. Water Pump Efficiency Chart.

Table 6. Pump Sizing Table.

Pump size (gal/m) at 20psi(14.1 m of head)	Height (mm)	Width (m)	Top Speed (mph)
90.00	10.00	1.00	1.27
90.00	5.00	1.00	2.54
90.00	10.00	0.75	1.70
90.00	5.00	0.75	3.39
90.00	10.00	0.50	2.54
90.00	5.00	0.50	5.09
90.00	10.00	0.25	5.09
90.00	5.00	0.25	10.17
100.00	10.00	1.00	1.41
100.00	5.00	1.00	2.83
100.00	10.00	0.75	1.88
100.00	5.00	0.75	3.77
100.00	10.00	0.50	2.83
100.00	5.00	0.50	5.65
100.00	10.00	0.25	5.65
100.00	5.00	0.25	11.30
125.00	10.00	1.00	1.77
125.00	5.00	1.00	3.53
125.00	10.00	0.75	2.35
125.00	5.00	0.75	4.71
125.00	10.00	0.50	3.53
125.00	5.00	0.50	7.06
125.00	10.00	0.25	7.06
125.00	5.00	0.25	14.13

Table 7. Miller Bobcat 250 3-Phase Specifications.

Welding Mode	Process	Amp/Volt Ranges	Weld Output Rated at 100% Duty Cycle (at 104° F/40° C)	Generator Power	Sound Levels at Rated Output, 7 m (23 ft)	Dimensions	Net Weight
CV/DC	MIG/FCAW	19–28 V	200 A at 20 V	Single-Phase **Peak:** 10,500 watts **Continuous:** 9500 watts 120/240 VAC, 84/42 A Three-Phase **Peak:** 11,000 watts **Continuous:** 10,000 watts 480 V, 13 A	75.5 dB (100.5 Lwa)	H: 33 in (838 mm) W: 20 in (508 mm) D: 45-1/2 in (1156 mm)	540 lb (245 kg)
CC/DC	Stick/TIG	50–210 A	210 A at 25 V				
CC/AC	Stick/TIG	50–225 A	225 A at 25 V				

Appendix B – Test Trailer Capability Sheet

Loading Mechanism:

- Air Spring loading with maximum of 8630 lbf at installed height.
- Linear bearing slide plate to accommodate different tire sizes.

Tire Geometry Capabilities:

- Tire diameters from 23 in. to 38 in.
- Camber adjustment of -10 to +10 degrees by way of 6 inch stroke Duff-Norton Mechanical actuator.
- Slip angle sweep of -16 to +16 degrees by way of Parker-Hannifin servo motor.
- Slip ratio testing expansion capability.

Wet Testing:

- Onboard 500 gallon tank provides wet testing capabilities.
- Maximum 10mm water depth can be provided during test runs.

Force Hub:

- Kistler 3-axis piezoelectric force and moment hub.
- Hub can accept any wheel size with the use of adapter plates.
- Hub contains sensors for forces and moments about all 3 axes.

Geometry Sensors:

- Linear potentiometers are used for accurate gauging of camber angles.

Data Acquisition:

- National Instruments LabView is used to collect and store data during test runs from all sensors and force hub.

- LabView also can provide a control method for load compensation during test run.

Test Outputs:

- Slip angle sweep data at discrete camber angles.
- Lateral force and overturning moment versus camber angle.
- Lateral force and aligning torque versus slip angle.
- Lateral force and longitudinal force versus slip ratio capability.

Appendix C – TTT CAD Drawings

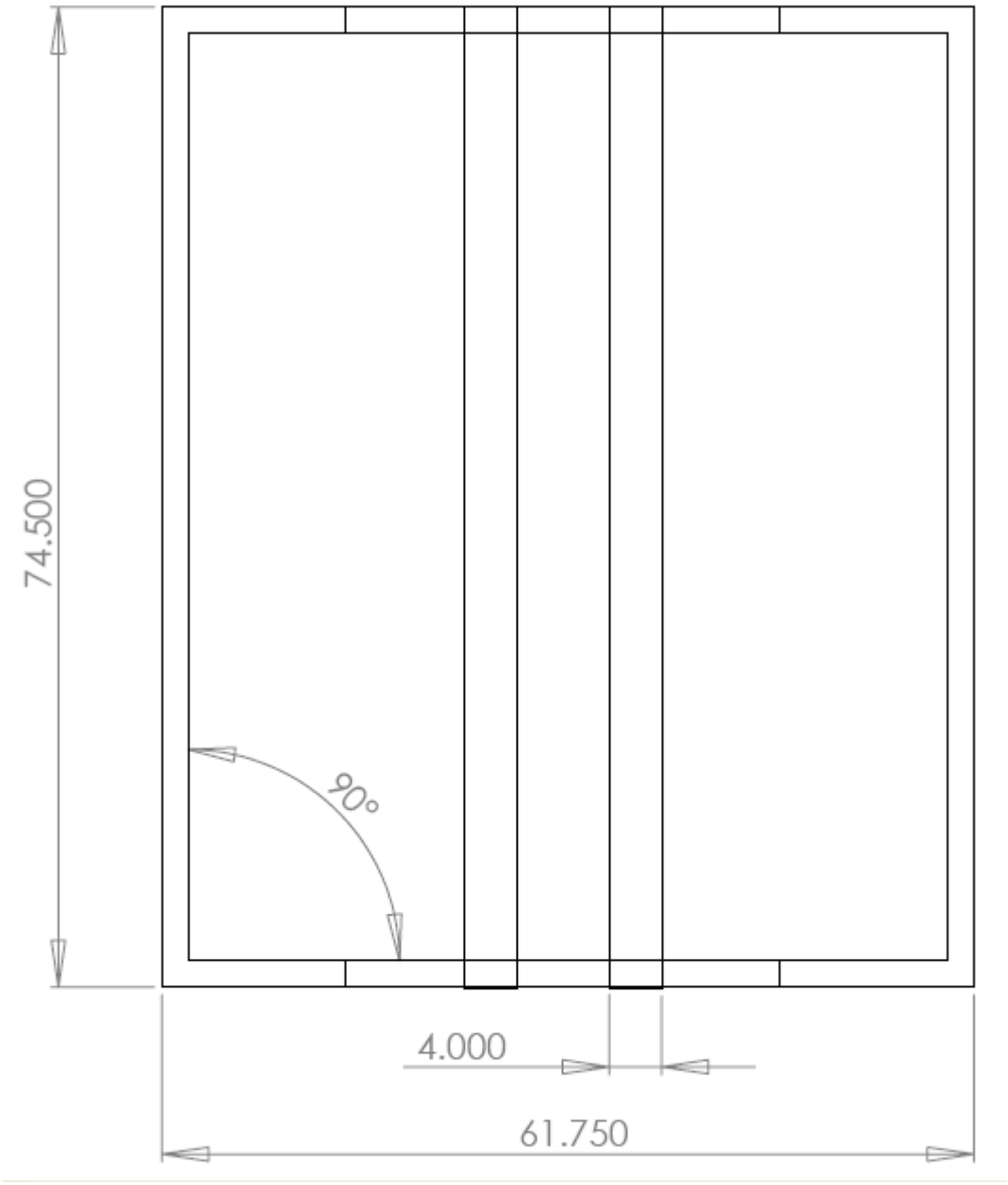

Figure 50. Frame Top View

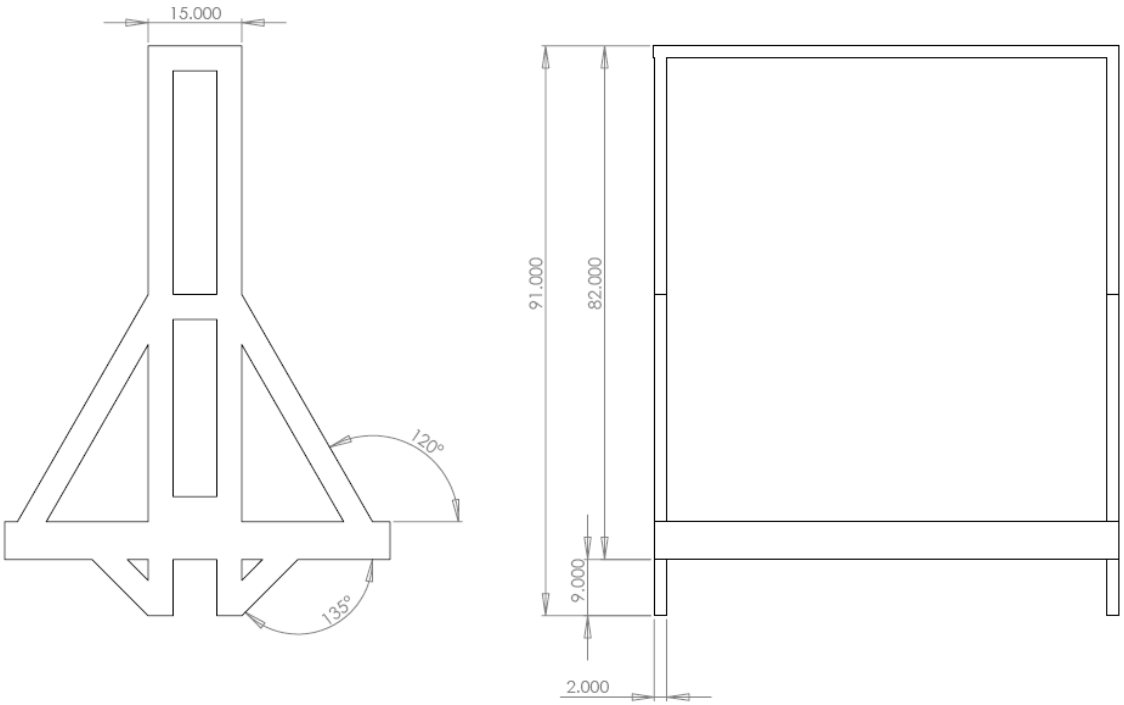

Figure 51. Alternate Frame Views

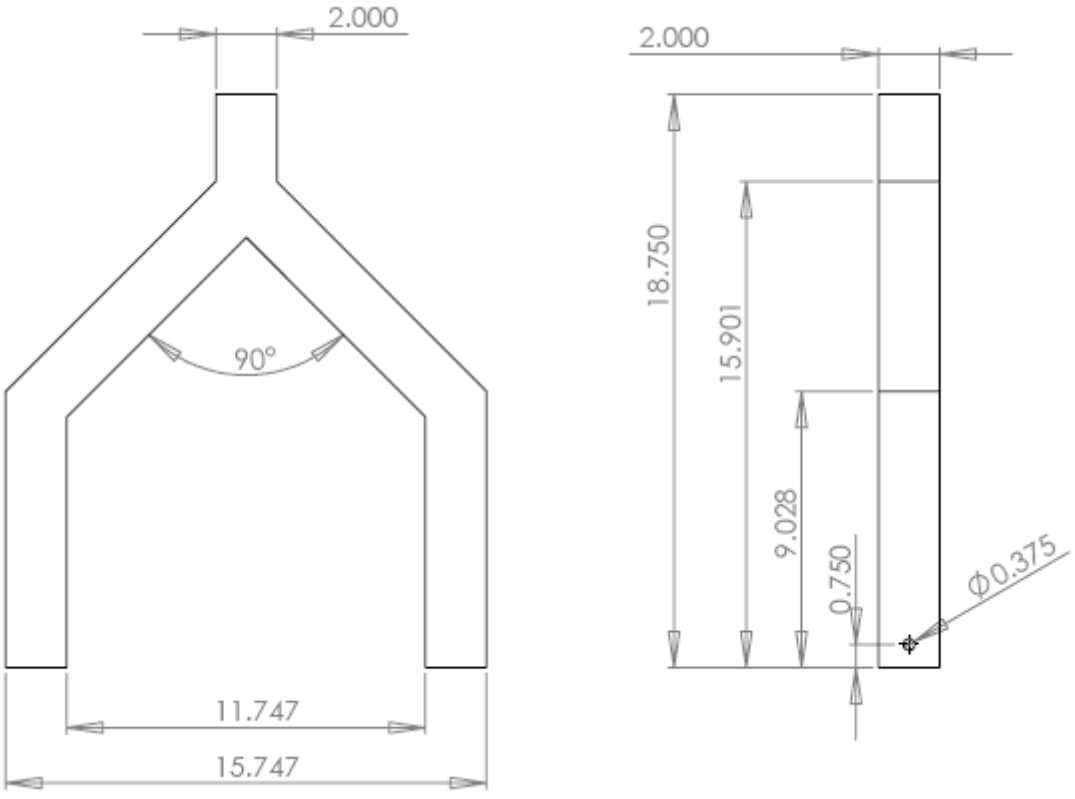

Figure 52. Steering Fork

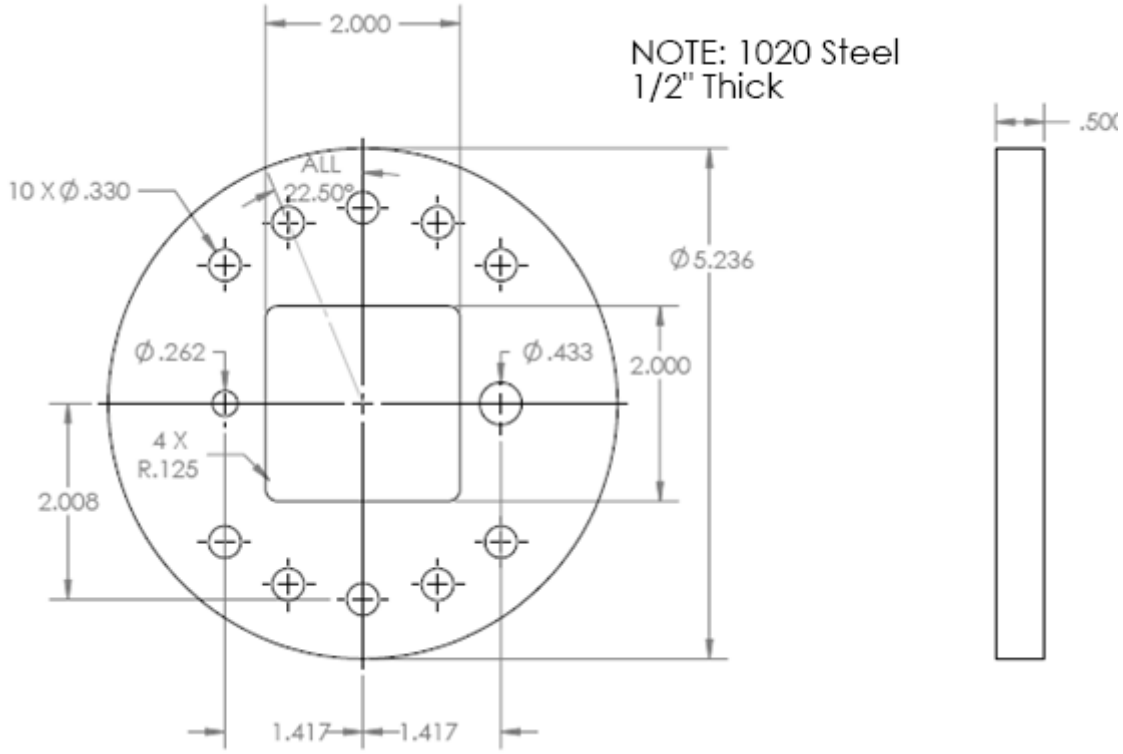

Figure 53. Steering Fork Mount Plate

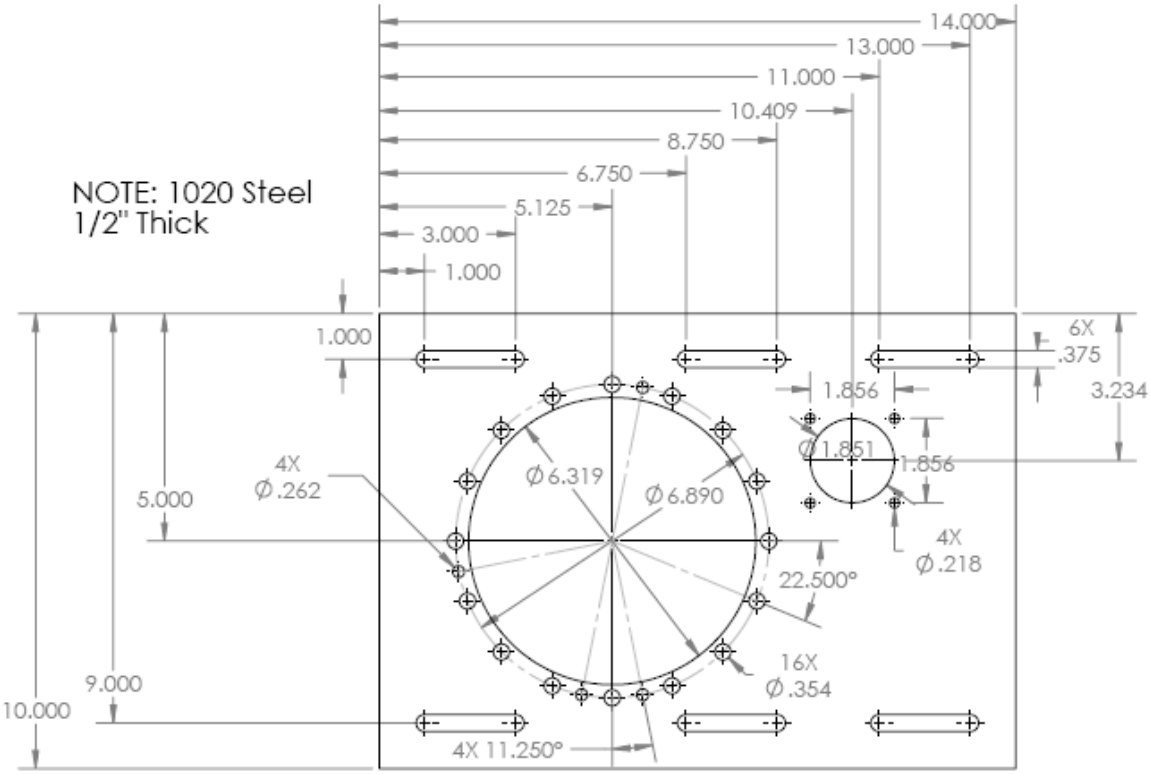

Figure 54. Steering Gearhead Mount Plate

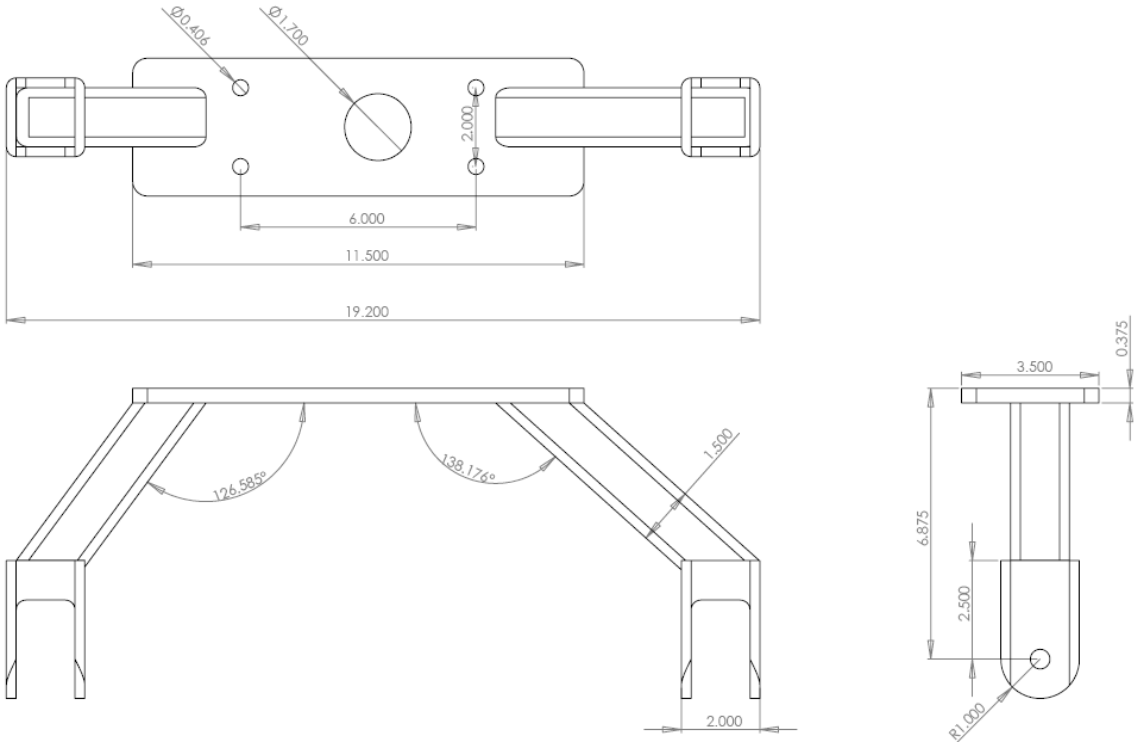

Figure 55. Upper Suspension Link

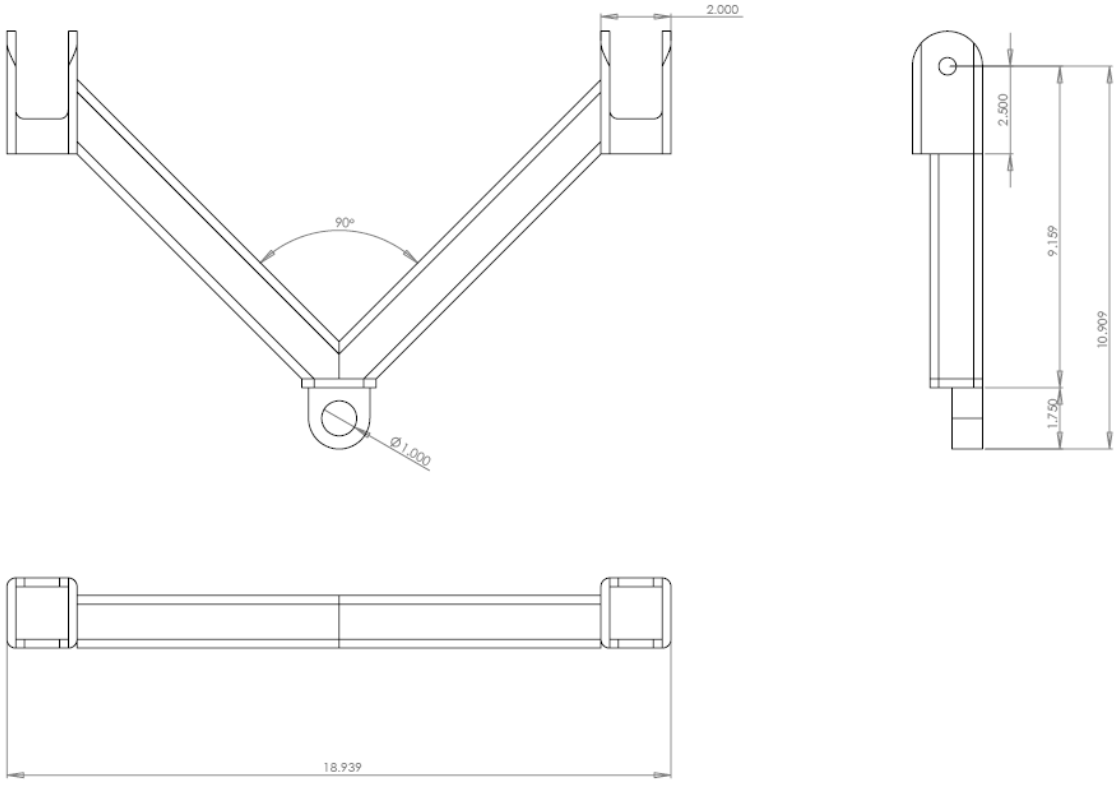

Figure 56. Lower Suspension Link

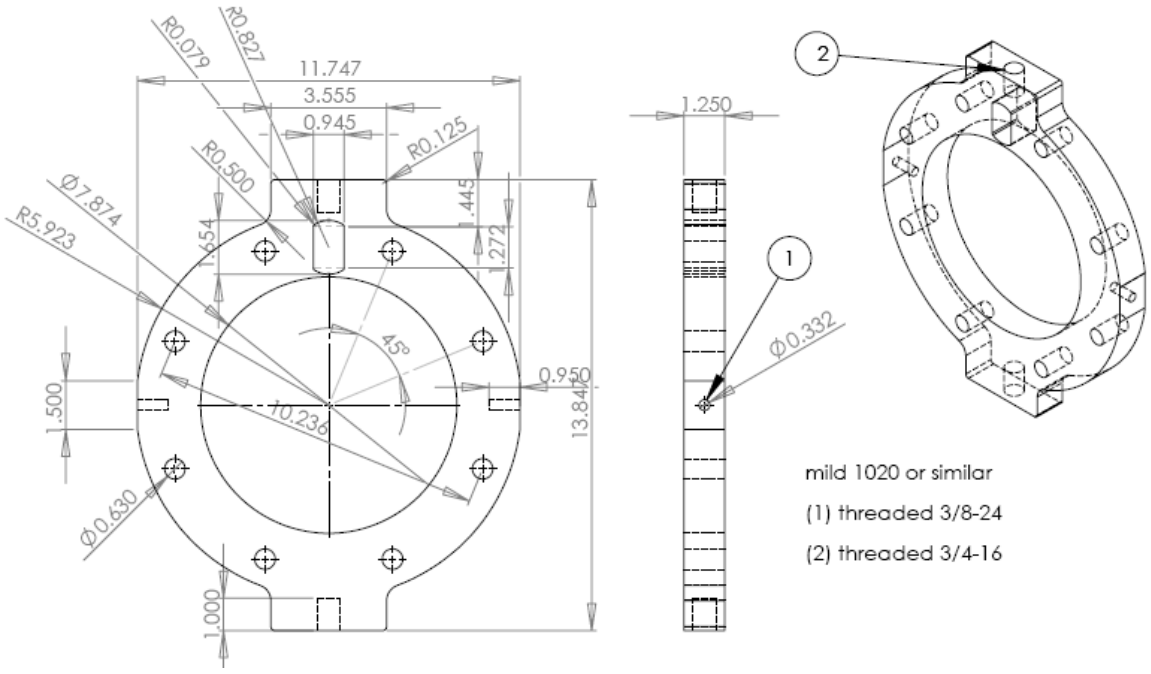

Figure 57. Force Hub Mounting Plate